

We are IntechOpen, the world's leading publisher of Open Access books Built by scientists, for scientists

5,800

Open access books available

142,000

International authors and editors

180M

Downloads

Our authors are among the

154

Countries delivered to

TOP 1%

most cited scientists

12.2%

Contributors from top 500 universities



WEB OF SCIENCE™

Selection of our books indexed in the Book Citation Index
in Web of Science™ Core Collection (BKCI)

Interested in publishing with us?
Contact book.department@intechopen.com

Numbers displayed above are based on latest data collected.
For more information visit www.intechopen.com



Can We Entangle Entanglement?

Mrittunjoy Guha Majumdar

Abstract

In this chapter, nested multilevel entanglement is formulated and discussed in terms of *Matryoshka* states. The generation of such states that contain nested patterns of entanglement, based on an anisotropic XY model has been proposed. Two classes of multilevel-entanglement- the *Matryoshka Q-GHZ states* and *Matryoshka generalised GHZ states*, are studied. Potential applications of such resource states, such as for quantum teleportation of arbitrary one, two and three qubits states, bidirectional teleportation of arbitrary two qubit states and probabilistic circular controlled teleportation are proposed and discussed, in terms of a *Matryoshka* state over seven qubits. We also discuss fractal network protocols, surface codes and graph states as well as generation of arbitrary entangled states at remote locations in this chapter.

Keywords: Quantum Computation, Multipartite Entanglement, Quantum State Sharing

1. Introduction

Quantum Entanglement is a fundamental non-classical aspect of entities in the quantum realm, which disallows a reductionist description of a composite system - in terms of the state and properties of its quantum constituents. Erwin Schrodinger once famously said,

“Thus one disposes provisionally until the entanglement is resolved by actual observation of only a common description of the two in that space of higher dimension. This is the reason that knowledge of the individual systems can decline to the scantiest, even to zero, while that of the combined system remains continually maximal. The best possible knowledge of a whole does not include the best possible knowledge of its parts—and this is what keeps coming back to haunt us”

Albert Einstein, Boris Podolsky and Nathan Rosen, famously known as EPR, and Schrödinger, who called it *Verschränkung*, highlighted the intrinsic order of statistical relations between the constituents of a compound quantum system, first recognised what they called a ‘spooky’ feature of the quantum world. John Bell showed that it is entanglement which irrevocably rules out the possibility of ascribing values to physical quantities of entangled systems prior to measurement. He accepted the EPR conclusion around the quantum description of nature not being ‘complete’, with the principles of ‘realism’ (measurement results are determined by properties that the particles carry prior to, and are independent of, the measurement), ‘locality’ (measurements obtained at one location are independent of any actions performed at another point that is spacelike separated) and ‘free will’ (settings of a local apparatus are independent of what EPR called ‘hidden variables’

that determine the local results) being primary in this discussion. Bell showed that if one were to assume these principles, then one obtains constraints in the form of certain inequalities, called Bell's Inequalities, on the statistical correlations in the measured values of properties of the systems, and that the probabilities of the outcomes of a measurement performed on constituents of an entangled system violate the Bell inequality. In this manner, it was shown that entanglement makes it impossible to simulate quantum correlations within the classical manner of thinking. Greenberger, Horne, and Zeilinger (GHZ) went beyond two particles in showing entanglement of quantum particles leads to contradictions with *Local Hidden Variables Models (LVHM)* for non-statistical predictions of quantum systems. During his doctoral studies at Université d'Orsay, Alain Aspect performed the first experimental realisation of the Bell's Inequalities.

Today, entanglement is instrumental in the formulation of information processing tasks in the quantum realm. It has been used in applications such as superdense coding and teleportation. *Bennett et al* first proposed a scheme for quantum teleportation, wherein a genuinely entangled Bell state was used to transmit an arbitrary single qubit [1]. Many different kinds of entangled quantum states have been used to teleport arbitrary quantum states since then, including Bell states [2, 3], GHZ states [4, 5], W states [6, 7] and multiqubit states [8–10]. There have been hop-by-hop and multi-hop quantum teleportation schemes proposed since then as well as schemes to teleport GHZ-like states using two types of four-qubit states [11, 12]. Teleportation has been proposed in two-copy quantum teleportation scheme [13], using cluster states [14], in higher dimensions [15] and also shown to be possible over atmospheric channels [16]. More recently, various derivatives of the standard teleportation scheme have been proposed, including those used for bidirectional teleportation [15, 17, 18], controlled teleportation [19, 20], quantum operation sharing [21, 22], quantum secret sharing [23–25] and arbitrated quantum teleportation [26, 27]. For multiple participants in a quantum information processing task, entangled multiqubit states and multipartite entanglement play the preeminent role, with multiqubit resource states varying from GHZ- and W-states to clusters states [28]. Lately, W-GHZ composite states have been used for remote state preparation, teleportation and superdense coding of arbitrary quantum states [29, 30]. *Shuai et al* showed how GHZ-GHZ channels can be used for bidirectional quantum communication [31]. The physical realisation of such composite systems have been explored in a number of physical platforms such as using cavity QED [32]. Properties of spin squeezing when multi-qubit GHZ state and W state are superposed have also been studied [33]. These composite quantum states contain varying degrees of multilevel and genuine multipartite entanglement, which can be used for applications in quantum information processing [34, 35]. *Yang et al* investigated the feasibility of experimentally creating GHZ states comprising of three logical qubits in a decoherence-free subspace, by using superconducting transmon qutrits coupled to a co-planar waveguide resonator [36].

Since not all forms of entanglement are relevant for distinct information processing applications, the determination of resource states for specific information processing tasks is of paramount importance. This, along with any characteristic protection or resilience against noise and decoherence provided by a resource state, forms the underlying principle of quantum resource theories [37–40]. In the latter pursuit, decoherence-free subspaces provide a natural solution and associated resources to produce quantum resource-states that are not easily decohered [41–44]. Stabiliser codes are a resource that constitutes a crucial ingredient for effective quantum error correction [45], while cluster states are resource states that are used for measurement-based quantum computation and error corrections [46–51]. Certain realisations of a standard resource-state have more resilience against decoherence,

such as in the case of cluster states generated with Ising-type interactions, wherein the entanglement in the state persisted upto a fairly large number of measurements on the qubits to disentangle them [52]. These resource state display various distinct forms of entanglement: some are maximally entangled, such as resource-states used for teleportation, while others are partially entangled, such as in the case of cluster states. In the case of cluster states, the partial entanglement is a resource in itself, since the one requires a specific protection of the ‘quantumness’ and correlations in the segments of the state against perturbations or measurements of other segments of the state. If the resource-state were maximally entangled, such a measurement or perturbation of one segment will collapse the state of the remaining segments to a specific state, thereby not maintaining the system as a viable quantum resource for further cluster operations. If we were to generalise and extend this idea to conceptualise states that maintain near maximal entanglement in segments of the state while maintaining weak correlations between the segments, we could have interesting resource-states and associated applications of such states. This is the central idea and motivation behind generalising the concept of *Matryoshka* states: *Matryoshka Generalised GHZ* states, *Matryoshka GHZ-Bell* States and *Matryoshka Q-GHZ* States.

In multi-qubit quantum states, an important property is that entanglement is monogamous - quantum entanglement cannot be shared freely among various parties. *Osborne and Verstraete* showed that the entanglement for bipartitions over an n-qubit system follows a monogamy relation [53]:

$$\tau(\rho_{A_1A_2}) + \tau(\rho_{A_1A_3}) + \dots + \tau(\rho_{A_1A_n}) \leq \tau(\rho_{A_1(A_2 \dots A_n)}) \quad (1)$$

where $\tau(\rho_{A_1(A_2 \dots A_n)})$ denotes the bipartite quantum entanglement measured by the tangle across the bipartition $A_1 : A_2A_3 \dots A_n$. In this chapter, we discuss the weak coupling between near-maximally entangled (sub)states due to the constraint placed by entanglement monogamy [54–57]. The concept of *Matryoshka* states was first given by *Di Franco et al* [58], with the name ‘*Matryoshka*’ coming from the Russian word for ‘nesting doll’. The underlying concept of a *Matryoshka* state is genuine entanglement in multilevel systems, with the entanglement in higher level systems being more than or equal to the entanglement in the lower level constituents:

$$E_{d_i} \geq E_{d_j}, d_i > d_j \quad (2)$$

where E_{d_i} is the entanglement measure of the level d_i . In this chapter, we will discuss the characteristics and applications of two classes of *Matryoshka* states for $d = 2$ multiqubit systems, which are as follows:

1. *Matryoshka Generalised GHZ states*

$$|\psi_{MGHZ}\rangle = \sum_{k=1}^L \lambda_k |GHZ_{d_1}^{a_k, d_1, \pm}\rangle \dots |GHZ_{d_N}^{a_k, d_N, \pm}\rangle \quad (3)$$

$$\langle GHZ_{d_i}^{a_k, d_i, \pm} | GHZ_{d_i}^{a_{k'}, d_i, \pm} \rangle = \delta_{kk'} \forall i \quad (4)$$

A particular case of such states are the *Matryoshka GHZ-Bell states*

$$|\psi_{MGHzB}\rangle = \sum_{k=1}^L \lambda_k |GHZ_{d_1}^{a_k, d_1, \pm}\rangle |B_{d_2}^{a_k, d_2, \pm}\rangle \dots |B_{d_N}^{a_k, d_N, \pm}\rangle \quad (5)$$

where $|B\rangle$ signifies a Bell state.

$$\langle GHZ_{d_1}^{a_k, d_1, \pm} | GHZ_{d_1}^{a_{k'}, d_1, \pm} \rangle = \delta_{kk'} \forall i \quad (6)$$

$$\langle B_{d_i}^{a_k, d_i, \pm} | B_{d_i}^{a_{k'}, d_i, \pm} \rangle = \delta_{kk'} \forall i \quad (7)$$

2. Matryoshka Q-GHZ states

$$|\psi_{ME\text{ex}G}\rangle = \sum_{k=1}^L \lambda_k |A_1^k\rangle |GHZ_{d_2}^{a_k, d_2, \pm}\rangle \dots |GHZ_{d_N}^{a_k, d_N, \pm}\rangle \quad (8)$$

$$\langle GHZ_{d_i}^{a_k, d_i, \pm} | GHZ_{d_i}^{a_{k'}, d_i, \pm} \rangle = \delta_{kk'} \forall i, \langle A_1^k | A_1^{k'} \rangle = \delta_{kk'} \quad (9)$$

where $|A\rangle$ are orthogonal states that are eigenstates in the Z-basis for all qubits in the state. Here the subscript ' d_i ' in $|GHZ_{d_i}^{a_k, d_i, \pm}\rangle$ denotes the number of qubits in the i^{th} subsystem, while a is the decimal representation of the superposed term in the GHZ-like state that has the lowest decimal representation and \pm denotes the relative phase between the terms in superposition. GHZ-like states are the states that can be created from the GHZ state using local unitary operations. So, for instance, in a three-qubit system $|GHZ^{2,+}\rangle = \frac{1}{\sqrt{2}}(|010\rangle + |101\rangle)$ can be created from $|GHZ\rangle = \frac{1}{\sqrt{2}}(|000\rangle + |111\rangle)$ using $I_{2 \times 2} \otimes \sigma_x \otimes I_{2 \times 2}$, or in other words - we apply a qubit flip σ_x operation on the second qubit, leaving the other qubits untouched. In the summation above, $L = 2^{n_h}$ where n_h is the number of qubits in the largest subsystem.

Nomenclature and Acronyms Used. GHZ state is a multipartite maximally entangled state, first defined for three qubits: $|\psi_{\pm}\rangle = \frac{1}{\sqrt{2}}(|000\rangle \pm |111\rangle)$. A Hadamard Operator is a quantum logical gate that acts on a single qubit and maps the basis state $|0\rangle$ to $\frac{|0\rangle + |1\rangle}{\sqrt{2}}$ and $|1\rangle$ to $\frac{|0\rangle - |1\rangle}{\sqrt{2}}$.

2. Localised correlation generation: how can we generate entangled entanglement?

Matryoshka states can be generated in various physical platforms, such as in spin systems and in trapped ions. Fröwis and Dür [59] studied the stability of superpositions of macroscopically distinct quantum states under decoherence, wherein they looked at realising concatenated-GHZ states: $|\phi_C\rangle = \frac{1}{\sqrt{2}}(|GHZ_m^+\rangle^{\otimes N} + |GHZ_m^-\rangle^{\otimes N})$ (with $|GHZ_N^{\pm}\rangle = \frac{1}{\sqrt{2}}(|0\rangle^{\otimes N} \pm |1\rangle^{\otimes N})$), which is a Matryoshka generalised state state, in trapped ion systems. The underlying principle to realise entangled entanglement is to have localised and intra-level correlation generation, which begins with creation of entanglement in one level, thereafter entanglement of this entangled structure over higher-level basis states and so on. For the purposes of this chapter, we will be considering the GHZ and GHZ-like states as the primary unit of entanglement.

The algorithm for generating entangled entanglement in a system comprising of GHZ and GHZ-like states as the units of entanglement is given by

Step 1: Creation of a ground state $|0000\dots 0\rangle$ with total number of qubits being $n = 3k$ for some finite, non-vanishing integer k .

Step 2: Application of a Hadamard gate on the $(3n + 1)^{\text{th}}$ qubits to give $|+ 00 + \dots 0\rangle$ where $|+\rangle = \frac{1}{\sqrt{2}}(|0\rangle + |1\rangle)$.

Step 3: Application of CNOT operation with the $(3n + 1)^{\text{th}}$ qubits as the control for the corresponding $(3n + 2)^{\text{th}}$ qubits and $(3n + 3)^{\text{th}}$ qubits as target to give a state of the form $|GHZ^{(123)}\rangle|GHZ^{(456)}\rangle \dots |GHZ^{(n-2,n-1,n)}\rangle$.

Step 4: Application of composite operation of the form of $\sum_{i=0}^{n/3} P_{3i+1}P_{3i+2}P_{3i+3}$ where P represents Pauli operations or combination of Pauli operations such as $\sigma_x\sigma_z$ and

$$1. P_{3i+1} \neq P_{3j+1} \text{ for } i \neq j \forall i, j \in \mathbb{Z}$$

$$2. P_{3i+2} \neq P_{3j+2} \text{ for } i \neq j \forall i, j \in \mathbb{Z}$$

$$3. P_{3i+3} \neq P_{3j+3} \text{ for } i \neq j \forall i, j \in \mathbb{Z}$$

2.1 Generation of Matryoshka states using spin systems in condensed matter physics

In this chapter, the generation of Matryoshka states will be explored in spin systems in condensed matter physics. Unlike in the case of the aforementioned algorithm, instead of composite operators, in this case we have localised generation and minimal interactions between different GHZ and GHZ-like states to create the Matryoshka states. In this case, we consider N spin- $\frac{1}{2}$ particles, with each spin coupled to its nearest neighbours by the XY Hamiltonian

$$H = \sum_{i=1}^{N-1} (J_{X,i} \hat{X}_i \hat{X}_{i+1} + J_{Y,i} \hat{Y}_i \hat{Y}_{i+1}) \quad (10)$$

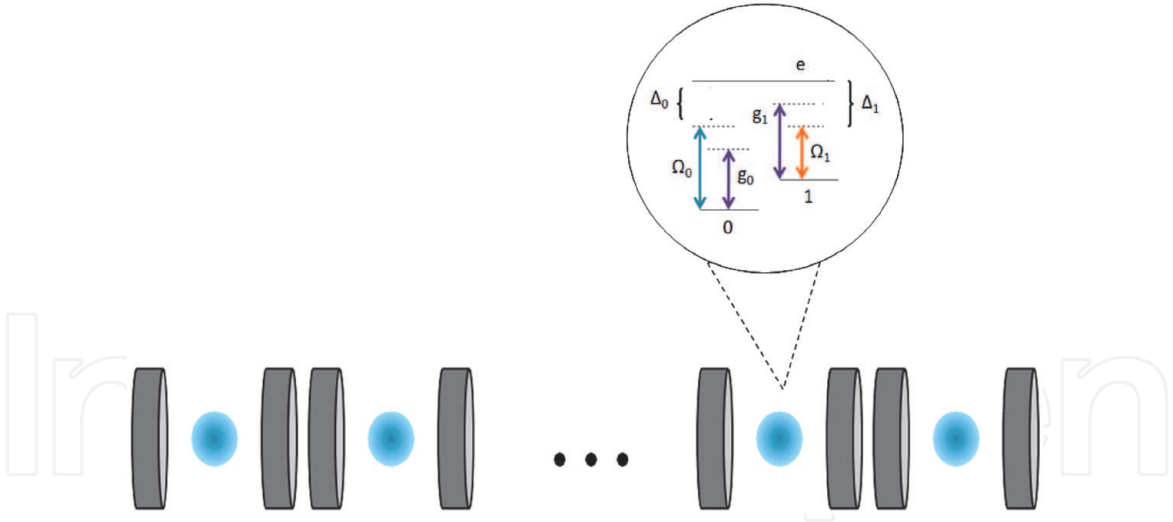
where $J_{\sigma,i}$ is the pairwise coupling constant with $\sigma = \hat{X}, \hat{Y}, \hat{Z}$ being the Pauli operators. For the purposes of this chapter, we take N to be odd. *Franco et al* [58] showed that it is sufficient to state that the information flux between the \hat{X} (\hat{Y}) operators of the first and last qubits in the spin-chain depends on an alternating set of coupling strengths. For example, the information flux from \hat{X}_1 to \hat{X}_N depends only on the set $\{J_{Y,1}, J_{X,2}, \dots, J_{Y,N-1}\}$ and is independent of any other coupling rate in the spin-chain. *Christandl et al* [60, 61] showed that after a time $t^* = \pi/\lambda$ with λ being a scaling constant (as mentioned in the definition of the case of a perfect state transfer in a linear spin-chain given by weighted coupling strengths: $J_{\sigma,i} = \lambda\sqrt{i(N-i)}$), the state of the first qubit in the spin-chain can be perfectly transferred to the last qubit. We see that by preparing the initial state of this spin-chain in an completely separable eigenstate of the tensorial product of Z_i operators, say $|\Psi(0)\rangle = |000\dots 0\rangle_{12\dots N}$, we obtain an information flux towards symmetric two-site spin operators, and a final state of the form [58].

$$|\psi_0\rangle = |0\rangle_c \otimes_{i=0}^M |\psi_+\rangle_{2i+1, N-2i} \otimes_{i=1}^M |\psi_-\rangle_{2i, N-2i+1} \quad (11)$$

$$|\psi_1\rangle = |1\rangle_c \otimes_{i=0}^M |\psi_-\rangle_{2i+1, N-2i} \otimes_{i=1}^M |\psi_+\rangle_{2i, N-2i+1} \quad (12)$$

where c labels the central site of the spin-chain, $M = \frac{N-3}{4}$ and $|\psi_{\pm}\rangle = \frac{1}{\sqrt{2}}(|00\rangle \pm |11\rangle)$. An illustration of the setup has been shown in **Figure 1**.

The critical step in the creation of the Matryoshka GHZ-Bell state is the evolution of the central and two neighbouring qubits to the GHZ state, without disturbing the rest of the spin-chain. This is a key result around the generation of *Matryoshka* GHZ-Bell states in this chapter, which can be extended to other classes of *Matryoshka* states.


Figure 1.

Scheme for the generation of Matryoshka GHZ-Bell resource-states, where the effective spin–spin XY Hamiltonian is obtained as an effective adiabatic Hamiltonian for a linear chain of optical cavities with each interacting with a three-level atomic system. The ground states of each atomic unit provide the computational space of each spin, and the dipole-forbidden transition between these states is realised as an (adiabatic) Raman transition through the excited state: $|e\rangle_i$ with $i = 1, 2, \dots, N$. The cavity field drives off-resonantly the dipole-allowed channel $|j\rangle_i \leftrightarrow |e\rangle_i$ with the Rabi frequency g_j , $j = 0, 1$. Two lasers are also coupled to these atomic transitions with strength Ω_j and detuning Λ_j .

For this, we need to switch off all the interactions except for those connecting the central qubit to the neighbouring ones. A point to note here is that had we started with $|\Psi(0)\rangle = |111\dots 1\rangle_{12\dots N}$, we would have obtained a final state of the form

$$|\psi_0\rangle = |0\rangle_c \otimes_{i=0}^M |\psi_-\rangle_{2i+1, N-2i} \otimes_{i=1}^M |\psi_+\rangle_{2i, N-2i+1} \quad (13)$$

$$|\psi_1\rangle = |1\rangle_c \otimes_{i=0}^M |\psi_+\rangle_{2i+1, N-2i} \otimes_{i=1}^M |\psi_-\rangle_{2i, N-2i+1} \quad (14)$$

We use this principle and the idea that after evolution over time t^* , the states in Eqs. (2) and (3) transform back to $|000\dots 000\rangle_{12\dots N}$ and states in Eqs. (4) and (5) transform back to $|111\dots 11\rangle_{12\dots N}$. We can utilise this concept, by taking the state in Eq. (2) and evolving it, for the truncated subsystem comprising of the central qubit and the adjoining qubits. A point to note here is that due to only coupling that connects to the central qubits, the coupling strength ($J'_{\sigma,i} = \lambda' \sqrt{i(3-i)}$) and time of evolution ($t'' = \pi/\lambda'$) vary accordingly. Before carrying out this evolution, we perform a Hadamard operation on the central qubit to give

$$|\psi_0\rangle = \frac{1}{\sqrt{2}} (|0\rangle_c + |1\rangle_c) \otimes_{i=0}^M |\psi_+\rangle_{2i+1, N-2i} \otimes_{i=1}^M |\psi_-\rangle_{2i, N-2i+1} \quad (15)$$

We now perform the truncated subsystem time-evolution with the parameters (J', t'') to give us the state

$$|\psi_0\rangle = \frac{1}{\sqrt{2}} (|000\rangle + |111\rangle)_{c-1, c, c+1} \otimes_{i=0}^{M-1} |\psi_+\rangle_{2i+1, N-2i} \otimes_{i=1}^M |\psi_-\rangle_{2i, N-2i+1} \quad (16)$$

Therefore, we can obtain a Matryoshka GHZ-Bell state using nearest spin–spin interactions in a spin-chain. A similar generation protocol can be defined for the other two classes of Matryoshka states. The teleportation of an arbitrary n -qubit state can be performed using Matryoshka GHZ-Bell States [62].

Given the triangular three-qubit configuration, we can also consider the anisotropic Heisenberg Hamiltonian, which describes the interaction between three spins that are located at the corners of an equilateral triangle lying in the xy-plane, as shown in **Figure 2**.

$$H = -J_{xy} \sum_{i=1}^3 (S_i^x S_{i+1}^x + S_i^y S_{i+1}^y) - J_z \sum_{i=1}^3 S_i^z S_{i+1}^z + H_z \quad (17)$$

here the three spins S_i , with $S = 1/2$, are located at the corners $i = 1, 2, 3$, and $S_1 = S_4$. J_{xy} and J_z are the in-plane and out-of-plane exchange coupling constants respectively, and $H_z = \sum_{i=1}^3 b_i \cdot S_i$ denotes the Zeeman coupling of the spins S_i to the externally applied magnetic fields b_i at the sites i . If we consider isotropic exchange couplings: $J_{xy} = J_z = J > 0$ (ferromagnetic coupling) and $b_i = 0 \forall i$, we have a ground-state quadruplet that is spanned by the GHZ states: $\frac{1}{\sqrt{2}}(|000\rangle + |111\rangle)$ and $\frac{1}{\sqrt{2}}(|000\rangle - |111\rangle)$, along with the W- and spin-flipped W-states. A set of appropriately chosen magnetic fields will allow us to split off an approximate GHZ state from this degenerate eigenspace. If we find a set of magnetic fields that, in classical spin systems, shall result in exactly two degenerate minima for the configurations $|000\rangle$, representing the $\downarrow\downarrow\downarrow$ spin configuration, and $|111\rangle$, representing the $\uparrow\uparrow\uparrow$ spin configuration, with an energy barrier in between, quantum mechanical tunnelling shall yield the desired states. The magnetic fields must be of the same strength, in-plane and sum to zero, with a convenient additional choice being that of the field pointing radially outward. Therefore, the successive directions of the magnetic fields have to differ by an angle of $2\pi/3$ with respect to each other. Going by the schematic in **Figure 2**, we can write the hamiltonian

$$H = -J_{xy} \sum_{i=1}^3 (S_i^x S_{i+1}^x + S_i^y S_{i+1}^y) - J_z \sum_{i=1}^3 S_i^z S_{i+1}^z + H_z$$

$$+ \sum_{il=1}^{N_l} \left[-J_{xy}^{(il)} \sum_{i=1}^3 (S_i^x S_{i+1}^x + S_i^y S_{i+1}^y) - J_z^{(il)} \sum_{i=1}^3 S_i^z S_{i+1}^z + H_z^{(il)} \right]$$

$$+ \sum_{ir=1}^{N_r} \left[-J_{xy}^{(ir)} \sum_{i=1}^3 (S_i^x S_{i+1}^x + S_i^y S_{i+1}^y) - J_z^{(ir)} \sum_{i=1}^3 S_i^z S_{i+1}^z + H_z^{(ir)} \right]$$

$$+ \sum_{il=1}^{N_l} \lambda_{(il,il+1)}^l S_i^{n_l} \cdot S_{i+1}^{m_l} + \sum_{ir=0}^{N_r-1} \lambda_{(ir,ir+1)}^r S_i^{n_r} \cdot S_{i+1}^{m_r} \quad (18)$$

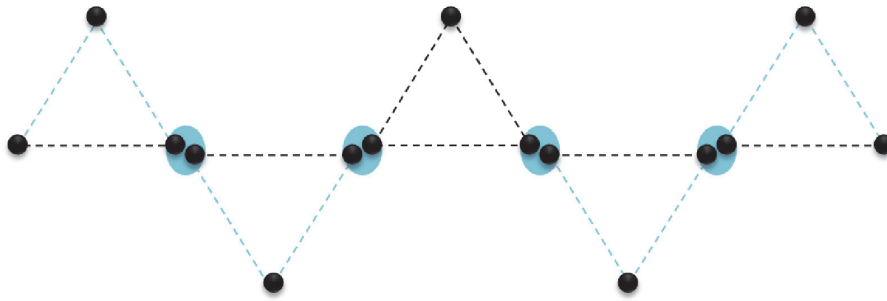


Figure 2. Schematic for all (three) classes of Matryoshka states for $d = 2$ levels of the quantum system, explored in this chapter. The triangular formations encapsulate the logical units of two/three qubits mediated by CNOT gates. Each of these triangular units are weakly coupled to each other (shown with light blue patches). In the case of the Matryoshka GHZ-Bell states, we only have the black links, while for the Matryoshka Generalised GHZ states and Matryoshka Q-GHZ states, we also have the blue links.

where the superscripts il and ir denote the left and right branches respectively of the schematic around a central triangular unit. For $il = 1$, we have the leftmost triangular unit and for $ir = N_r$, we have the rightmost triangular unit. N_l and N_r denote the number of units on the left and right side of the central triangular unit. In principle, we can have an asymmetric case where $N_l \neq N_r$. In the fourth line, the term S_{N_l+1} and S_0 refer to the spins in the central triangular unit connected to the adjacent left and right triangular units respectively. Moreover, both $\lambda_{(il,il+1)}^l$ and $\lambda_{(ir,ir+1)}^l$ are coupling constants between adjacent triangular units that are numerically negligible with respect to J but are non-zero, to account for inter-unit coupling. $S_i^{n_r}$ and $S_i^{m_l}$ are right and left connecting nodes of the i^{th} triangular unit.

An important point here is the condition: $\langle GHZ_{d_i}^{a_k, d_i, \pm} | GHZ_{d_i}^{a_{k'}, d_i, \pm} \rangle = \delta_{kk'} \forall i$, $\langle A_1^k | A_1^{k'} \rangle = \delta_{kk'}$ in Eqs. (4), (6) and (9). This is ensured by the additional application of single qubit gates on the nodes of the triangular units. For instance, $\frac{1}{\sqrt{2}}(|000\rangle + |111\rangle) \xrightarrow{\sigma_x^2} \frac{1}{\sqrt{2}}(|010\rangle + |101\rangle)$. Using combination of such single qubit operations, we can span the entire space of GHZ and GHZ-like states. The important point here is the synchronised timing of these operations, with the inter-unit coupling, so as to give us a superposition over orthogonal GHZ and GHZ-like states for all triangular units, as shown in **Figure 2**.

3. Creating tessellated networks of Matryoshka states

The Matryoshka Generalised GHZ states can also be oriented in a tessellated manner, as shown in **Figure 3(a)** for the case of symmetric 3-qubit GHZ triangular units. The Matryoshka GHZ-Bell states, a specific form of these states, can even be oriented in an emanatory manner, as shown in **Figure 3(b)**. These two orientations can be used for tessellation in three-dimensions, as in the case of the spherical configuration shown in **Figure 3(c)**, which shows the method of lattice surgery (discussed later in the chapter). More complex forms such as the hexagonal-pentagonal tiling with 6-qubit and 5-qubit GHZ states can be used for forms such as truncated icosahedrons. Lastly, we can also have higher GHZ-forms in a self-similar, fractal manner, as shown in **Figure 3(d)**. Each of these configurations will be studied in the *Application* section of this chapter. An interesting future direction of pursuing this line of research would be in squeezed baths, which *Zippilli et al* studied and showed that a squeezed bath, which acts on the central element of a harmonic chain, could drive the entire system to a steady state that features a series of nested entangled pairs of oscillators [63]. This series ideally covers the entire chain regardless of its size. Extending this result to higher number of nearest neighbour interactions is non-trivial.

4. Where can we use entangled entanglement?

Matryoshka states have a second level of entanglement (nesting) and have additional protection against loss of coherence under local transformations.

4.1 Fractal network protocol

In this chapter, a new quantum communication architecture is being proposed, whereby there are levels of entanglement which underly a distributed network. If we have

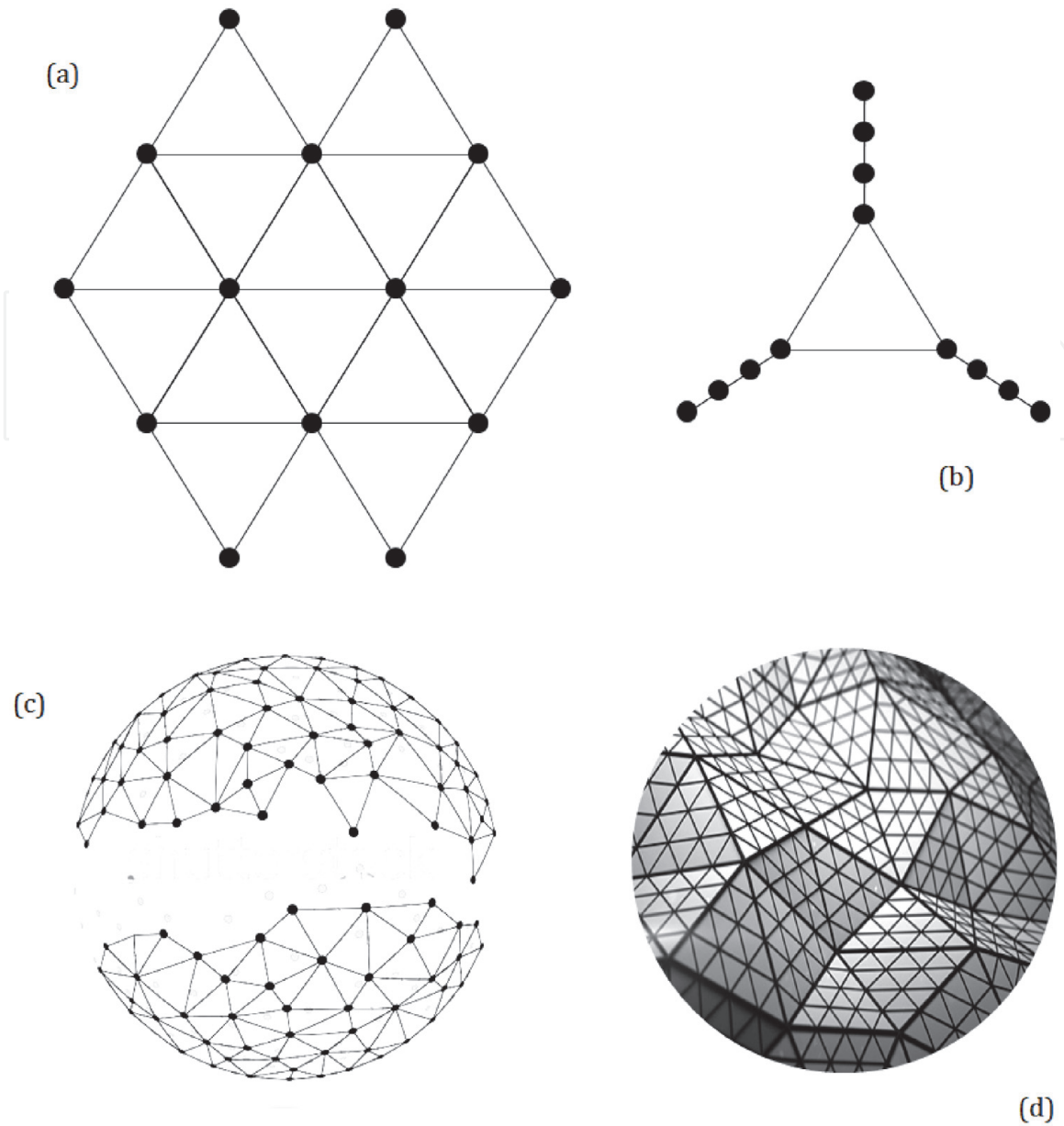


Figure 3. The various tessellation patterns possible with the GHZ triangular units in (a) generalised GHZ states in a planar tessellated format, (b) GHZ-Bell states with an emanatory geometry, (c) spherical pattern created by planar codes, along with illustration of lattice surgery with projective measurements, and (d) hierarchical GHZ-state levels, where we have a self-similar nature of the tessellation. A point to note here is that each node in the diagram has three physical qubits (one from each GHZ triangular unit) in the generalised GHZ states and two physical qubits in the GHZ-Bell states.

$$|0\rangle_L^n = \frac{1}{\sqrt{2}} (|0_L^{n-1} 0_L^{n-1} 0_L^{n-1}\rangle + |1_L^{n-1} 1_L^{n-1} 1_L^{n-1}\rangle) \quad (19)$$

$$|1\rangle_L^n = \frac{1}{\sqrt{2}} (|0_L^{n-1} 0_L^{n-1} 0_L^{n-1}\rangle - |1_L^{n-1} 1_L^{n-1} 1_L^{n-1}\rangle) \quad (20)$$

As you can see, these are special cases of Matryoshka Generalised GHZ states, with the superscript n defining the layer of the network. A point to note here is that $n = 1$ is the layer with physical qubits, and so $|0\rangle_L^1 = |0\rangle$ and $|1\rangle_L^1 = |1\rangle$. This effectively creates layers of *entangled entanglement*. This is highly useful in providing multiple levels of protection in quantum network encoding. The key point here is the heralded nature in which we can access levels from the highest to the lowest, with a projective measurement onto the basis logical qubits of the just-lower level of entanglement to pass through a level of entanglement-enabled security and robustness.

4.2 Surface codes, graph states and cluster states

We can define effective surface codes with Matryoshka states, with triangular units. The primary operation proposed to be utilised in this regard is that of lattice surgery and merging. Topological encoding of quantum data facilitates information processing to be protected from the effects of decoherence on physical qubits, by having a logical qubit encoded in the entangled state of many physical qubits. Among the various codes used for this purpose, the surface code has the highest tolerance of component error, when implemented on a two-dimensional lattice of spin-qubits with nearest-neighbour interactions [64–68]. Mhalla and Perdrix [69] proved that the application of measurements in the (X, Z) plane, with one-qubit measurement as per the basis

$$\{ \cos \theta |0\rangle + \sin \theta |1\rangle, \sin \theta |0\rangle - \cos \theta |1\rangle \} \quad (21)$$

for some θ over graph states that are represented by triangular grids, is a universal model of quantum computation. A point to note here is that, for any θ , the observable associated with the measurement in this basis is $\cos 2\theta Z + \sin 2\theta X$. For a given simple undirected graph $G = (V, E)$ of order n , where V represent vertices and E edges, the graph state $|G\rangle$ is the unique quantum state such that for any vertex $u \in V$,

$$X_u Z_{\mathcal{N}(u)} |G\rangle = |G\rangle \quad (22)$$

The Pauli operators constitute a group acting on a set V of n qubits is generated by $X_u, Z_u, i.I_{u \in V}$, where I is the identity, X_u and Z_u are operators that act as identity on the neighbourhood of u and with the following action on vertex u

$$X : |x\rangle \rightarrow |\bar{x}\rangle \quad (23)$$

$$Z : |x\rangle \rightarrow (-1)^x |\bar{x}\rangle \quad (24)$$

In our circuit, we will have to project three physical qubits from three adjacent triangular units to a single subspace for implementing this model. If we consider the state: $\frac{1}{2\sqrt{2}}(|00_c 0\rangle + |11_c 1\rangle)(|00_c 0\rangle + |11_c 1\rangle)(|00_c 0\rangle + |11_c 1\rangle)$, with the subscript c denoting the physical qubits adjacent to each other and that are projected to a single subspace. If we initialise an ancilla qubit in the state $|+\rangle = \frac{1}{\sqrt{2}}(|0\rangle + |1\rangle)$ and use the conditional rotation gate

$$U_\gamma = \begin{pmatrix} 1 & 0 & 0 & 0 \\ 0 & 1 & 0 & 0 \\ 0 & 0 & \cos \frac{\gamma}{2} & \sin \frac{\gamma}{2} \\ 0 & 0 & -\sin \frac{\gamma}{2} & \cos \frac{\gamma}{2} \end{pmatrix} \quad (25)$$

and apply this sequentially with the three adjacent physical qubits (with subscript 'c') and the ancilla as target, we project the ancilla to a unique state that can be retained for the graph state that is thereby defined, by going over the entire tessellated lattice of triangular GHZ-units.

4.3 Establishing multiparticle entanglement between nodes of a quantum communication network

We can use the unique form of the asymmetric Matryoshka Generalised GHZ states to establish multipartite entanglement between nodes of a quantum

communication network. The important part about this protocol is the role of projection measurements on a central terminal. Considering a Matryoshka GHZ-Bell state with an m -particle GHZ state and n -terminals in a quantum network

$$|\psi_{MGH\pm B}\rangle = \sum_{k=1}^L \lambda_k |GHZ_m^{a_k, m, \pm}\rangle |B_{d_1}^{a_k, d_1, \pm}\rangle \dots |B_{d_n}^{a_k, d_n, \pm}\rangle \quad (26)$$

where $|B\rangle$ signifies a Bell state, $\langle GHZ_m^{a_k, m, \pm} | GHZ_m^{a_{k'}, m, \pm} \rangle = \delta_{kk'}$ $\forall i$ and $\langle B_{d_i}^{a_k, d_i, \pm} | B_{d_i}^{a_{k'}, d_i, \pm} \rangle = \delta_{kk'}$ $\forall i$. Each user has one particle of a Bell-state, while the other particle of the Bell-state is with the central terminal. Measuring the particles of the Bell-pairs at the central terminal in a basis defined by maximally entangled states over n -qubits will project the distant qubits into maximally n -qubit entangled states as well. In fact, it need not only be one n -qubit maximally entangled state at the spatially distant nodes but could be multiple (partially or maximally) entangled states of varying number of qubits connecting different permutations of end-terminals, depending on the projective measurement performed on the central terminal. Some examples of such remote establishment of entanglement have been shown in **Figure 4**.

4.4 Quantum networks, repeater protocols and quantum communication

Quantum networks can facilitate the realisation of quantum technologies such as distributed quantum computing [70], secure communication schemes [71] and quantum metrology [72–75]. In our formalism for GHZ-based network protocols, the key element is that of being able to merge GHZ triangular units, which is done by projecting states at adjacent nodes into a single subspace (as shown in **Figure 5**), as has been tried on atomic systems previously [76]. A *generalised GHZ-GHZ Matryoshka state* can also assist in the recovery of quantum network operability upon node failure, based on the formalism given by *Guha Majumdar and Srinivas Garani* [77].

4.5 Teleportation and superdense coding

Let us look at the applications of such nested entanglement with the example of a state close to a Matryoshka Q-GHZ state: the Xin-Wei Zha (XZW) State. *Xin-Wei Zha et al* [78] discovered a genuinely entangled seven-qubit state through a numerical optimization process, following the path taken by *Brown et al* [79] and *Borras et al* [80] to find genuinely entangled five-qubit and six-qubit states:

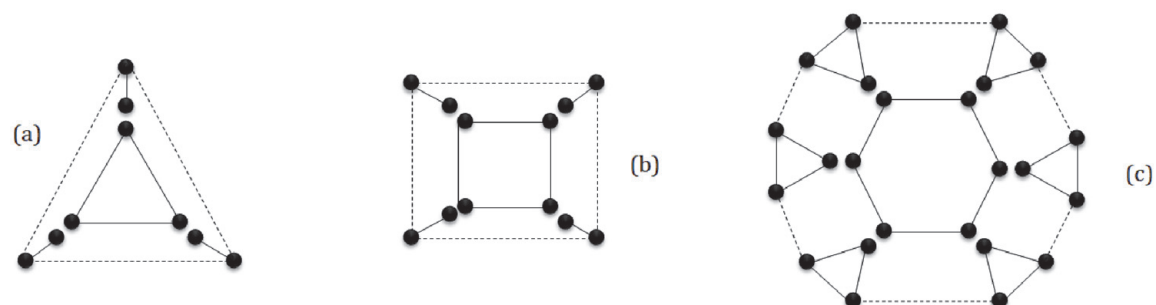


Figure 4. Illustration of networks for entanglement generation in remote nodes in (a) triangular format (b) rectangular format (c) polyhedra (dodecagon) format, with distinct patterns of entanglement generated at the periphery depending on the projective measurements at the central terminal(s).

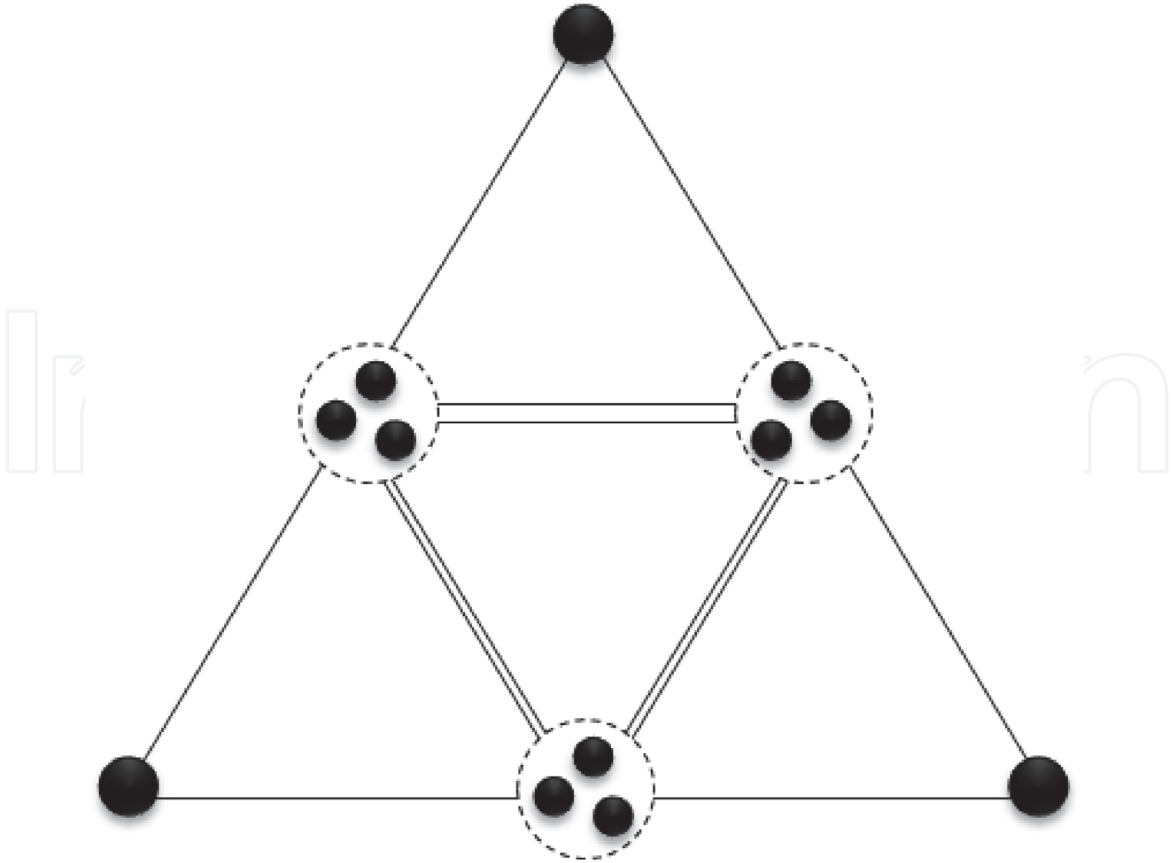


Figure 5.

Network repeater protocol with three-qubit projective measurements at nodes to create higher-distance entangled networks.

$$\begin{aligned}
 |\psi_7\rangle = & \frac{1}{2\sqrt{2}} (|000\rangle_{135} |\psi_+\rangle_{24} |\psi_+\rangle_{67} + |001\rangle_{135} |\phi_-\rangle_{24} |\phi_+\rangle_{67} \\
 & + |010\rangle_{135} |\psi_-\rangle_{24} |\phi_-\rangle_{67} + |011\rangle_{135} |\phi_+\rangle_{24} |\psi_-\rangle_{67} \\
 & + |100\rangle_{135} |\phi_+\rangle_{24} |\phi_+\rangle_{67} + |101\rangle_{135} |\psi_-\rangle_{24} |\psi_+\rangle_{67} \\
 & + |110\rangle_{135} |\phi_-\rangle_{24} |\psi_-\rangle_{67} + |111\rangle_{135} |\psi_+\rangle_{24} |\phi_-\rangle_{67})
 \end{aligned} \tag{27}$$

This state is a specific form of the Q-GHZ State defined in Eq. (6), with $\lambda_k \forall k = \frac{1}{2\sqrt{2}}$ and $|A_1^k\rangle \in \{|000\rangle, |001\rangle, |010\rangle, |011\rangle, |100\rangle, |101\rangle, |110\rangle, |111\rangle\}$. Another point to note here is that the GHZ states here are for $d = 2$, thereby effectively being the Bell states. This resource state can be used for teleportation of arbitrary single, double and triple qubit states. The 3 (Q State)-2 (Bell State)-2 (Bell State) structure of the resource-state, given in Eq. (17), helps us in devising a quantum circuit to generate the state, as shown in **Figure 6** and realised on *IBM Quantum Experience*. To obtain the resource-state, we apply a unitary operator on qubits 1, 3 and 5: $U = I_{4 \times 4} \oplus (\sigma_z \otimes \sigma_z)$.

This state has marginal density matrices for subsystems over one or two qubits that are completely mixed, with $\pi_{ij} = \text{Tr}_{ij} \rho_{ij}^2 = \frac{1}{4} \forall i, j \in \{1, 2, 3, 4, 5, 6, 7\}, i < j$, $\pi_i = \text{Tr}_i \rho_i^2 = \frac{1}{2} \forall i \in \{1, 2, 3, 4, 5, 6, 7\}$. For three-qubit subsystems, some of the partitions have mixed marginal density matrices: $\pi_{ijk} = \text{Tr}_{ijk} \rho_{ijk}^2 = \frac{1}{8} \forall i, j, k \in \{1, 2, 3, 4, 5, 6, 7\}, i < j < k \wedge (ijk) \neq (127), (367), (457)$ and $\pi_{127} = \pi_{367} = \pi_{457} = \frac{1}{4}$.

The seven-qubit genuinely entangled resource state $|\Gamma_7\rangle$ can be used for a number of applications, such as quantum secret sharing (*Supplementary Material A.1, A.2 and A.3*), the perfect linear teleportation of an arbitrary one-qubit state (*Supplementary Material B.1.1*), probabilistic circular teleportation of arbitrary one-

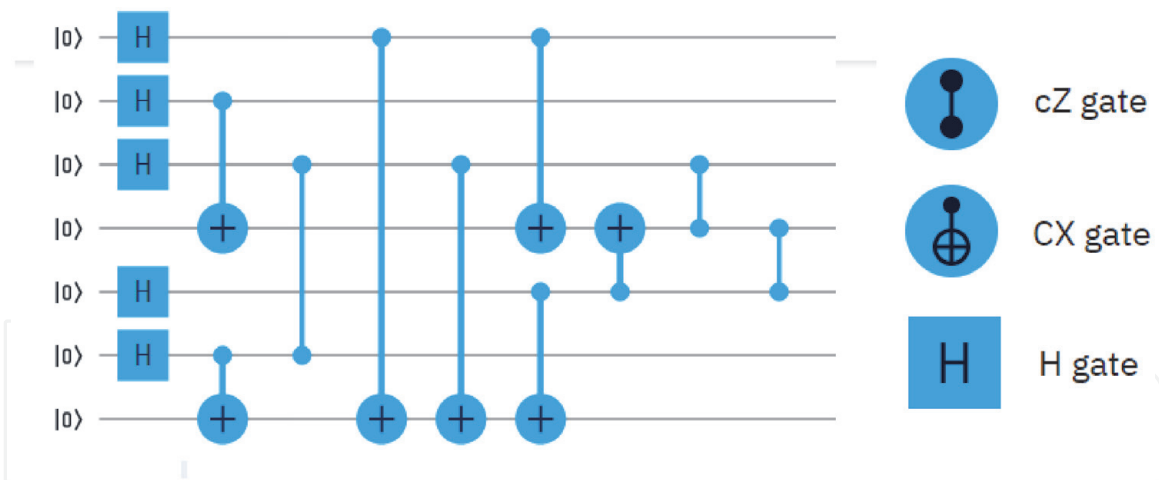


Figure 6. Quantum circuit for the generation of the seven-qubit genuinely entangled state, on IBM Quantum Experience. Here CX gate is the CNOT gate, cZ gate is the CPHASE gate and H gate is the Hadamard gate.

qubit states (Supplementary Material B.1.2), perfect linear teleportation of an arbitrary two-qubit state (Supplementary Material B.2.1), bidirectional teleportation of arbitrary two-qubit states (Supplementary Material B.2.2) and perfect linear teleportation of an arbitrary three-qubit state (Supplementary Material B.3).

5. Conclusion

In this chapter, the generation and application of nested entanglement in Matryoshka resource-states for quantum information processing was studied. A novel scheme for the generation of such quantum states has been proposed using an anisotropic XY spin-spin interaction-based model. The application of the *Matryoshka GHZ-Bell states* for n-qubit teleportation is reviewed and an extension of this formalism to more general classes of *Matryoshka states* is posited. An example of a state close to a perfect *Matryoshka Q-GHZ state* is given in the form of the genuinely entangled seven-qubit *Xin-Wei Zha state*. Generation, characterisation and application of this seven-qubit resource state is presented. This work should lay the groundwork for other studies into the area of nested entanglement, including forays into higher layers of nesting entanglement. Particularly, the problem of composite quantum states containing nested entanglement can be explored further, theoretically and experimentally, be it in surface codes, establishment of multipartite entanglement in quantum networks, teleportation, superdense coding and more broadly in quantum communication protocols. The main advantage of the model and method presented in this chapter is the accessibility of the condensed matter system presented, while the primary limitation of the model presented in this chapter is the need for fine-tuning of various interaction terms that have to be time-sequenced very carefully. The concept of entangled entanglement is the key result of the chapter, which can be implemented with other non-trivial combination of unitary transformations over multiple qubits.

Acknowledgements

I would like to acknowledge the guidance and contribution of Prof. Prasanta Panigrahi, IISER-Kolkata. This work was supported by the Homi Bhabha Centre for Science Education, Tata Institute of Fundamental Research, Mumbai, India.

Data availability statement

Data sharing is not applicable to this article as no new data were created or analysed in this study.

A. Quantum Secret Sharing

Quantum Secret Sharing (QSS) is a procedure for splitting a message into several parts so that no single subset of parts is sufficient to read the message, but the entire set is. This can also naturally be extended to Quantum Operation Sharing (QOS). In this section, quantum secret sharing using the 7 qubit XZW resource-state is proposed, with three proposals for the same.

A.1 Proposal 1

Let us consider the situation in which Alice possesses the 1st qubit, Bob possesses qubits 2, 3, 4, 5, 6 and Charlie possesses the 7th qubit. Alice has an unknown qubit $\alpha|0\rangle + \beta|1\rangle$ which she wants to share with Bob and Charlie.

Now, Alice combines the unknown qubit with $|\Psi_7\rangle$ and performs a Bell measurement, and conveys her outcome to Charlie by two classical bits. For instance if Alice measures in the $|\Phi_+\rangle$ basis, then the Bob-Charlie system evolves into the entangled state.

$$\begin{aligned}
 & \alpha|100001\rangle - \alpha|000100\rangle - \alpha|000111\rangle - \alpha|001001\rangle \\
 & + \alpha|001010\rangle + \alpha|010101\rangle - \alpha|010110\rangle - \alpha|011000\rangle \\
 & + \alpha|011011\rangle + \alpha|100010\rangle + \alpha|101100\rangle + \alpha|101111\rangle - \\
 & \alpha|110011\rangle + \alpha|111101\rangle - \alpha|111110\rangle + \beta|000000\rangle \\
 & + \beta|000011\rangle + \beta|001101\rangle + \beta|001110\rangle + \beta|010001\rangle \\
 & - \beta|010010\rangle + \beta|011100\rangle - \beta|011111\rangle - \beta|100101\rangle - \\
 & \beta|000000\rangle - \beta|100110\rangle + \beta|101000\rangle + \beta|101011\rangle \\
 & + \beta|110100\rangle - \beta|110111\rangle - \beta|111001\rangle + \beta|111010\rangle
 \end{aligned} \tag{A1}$$

Now, Bob can perform a five-qubit measurement and convey his outcome to Charlie through a classical channel. Having known the outcome of both their measurement, Charlie will obtain a certain single qubit quantum state. The outcome of the measurement performed by Bob is correlated with the state obtained by Charlie. If Bob measures $|A_\pm\rangle$ then Charlie obtains the state $\alpha|0\rangle \pm \beta|1\rangle$, while if Bob measures the state $|B_\pm\rangle$ then Charlie obtains the state $\beta|0\rangle \pm \alpha|1\rangle$, where

$$\begin{aligned}
 & |A_\pm\rangle \\
 & = -|00010\rangle + |00101\rangle - |01011\rangle - |01100\rangle \\
 & + |10001\rangle + |10110\rangle - |11111\rangle \pm (|00001\rangle \\
 & + |00110\rangle + |01000\rangle - |01111\rangle - |10010\rangle \\
 & + |10101\rangle - |11011\rangle - |11100\rangle)
 \end{aligned} \tag{A2}$$

$$\begin{aligned}
 |B_{\pm}\rangle &= \pm(|10000\rangle - |00011\rangle - |00100\rangle + |01010\rangle \\
 &+ |01101\rangle + |10111\rangle - |11001\rangle + |11110\rangle) \\
 &+ |00000\rangle + |00111\rangle - |01001\rangle + |01110\rangle \\
 &- |00000\rangle - |10011\rangle + |10100\rangle + |11010\rangle \\
 &+ |11101\rangle
 \end{aligned} \tag{A3}$$

A.2 Proposal 2

Let us consider the situation in which Alice possesses the qubits 1 and 2, Bob possesses qubits 3, 4, 5 and 6 and Charlie possesses the 7th qubit. Alice has an unknown qubit $\alpha|0\rangle + \beta|1\rangle$ which she wants to share with Bob and Charlie. Now Alice can measure in a particular basis. Suppose she measures in the GHZ Basis. Now, Bob can perform a four-qubit measurement and convey his outcome to Charlie through a classical channel. Having known the outcome of both their measurement, Charlie will obtain a certain single qubit quantum state. The outcome of the measurement performed by Bob and the state obtained by Charlie is given as follows: if Bob measures states $|x_{\pm}\rangle$, Charlie obtains states $\alpha|0\rangle \pm \beta|1\rangle$, while if Bob measures states $|Y_{\pm}\rangle$ then Charlie obtains the states $\beta|0\rangle \pm \alpha|1\rangle$, where $|x_{\pm}\rangle = \frac{1}{4}\alpha|0000\rangle + \alpha|0111\rangle + \alpha|1001\rangle + \alpha|1110\rangle \pm (\beta|1001\rangle + \beta|0000\rangle + \beta|1110\rangle - \beta|0111\rangle)$ and $|Y_{\pm}\rangle = \frac{1}{4}\alpha|0001\rangle + \alpha|0110\rangle + \alpha|1000\rangle - \alpha|1111\rangle \pm (\beta|1000\rangle + \beta|0001\rangle - \beta|1111\rangle - \beta|0110\rangle)$

A.3 Proposal 3

Let us consider the situation in which Alice possesses the qubits 1, 2, 3 and 4, Bob possesses qubits 5 and 6 and Charlie possesses the 7th qubit. Alice has an unknown qubit $\alpha|0\rangle + \beta|1\rangle$ which she wants to share with Bob and Charlie. Based on the state Alice measures ($|A_i\rangle \forall i \in \{1, 2, 3, 4, 5, 6, 7, 8\}$), Bob and Charlie obtain a corresponding state $|BC_i\rangle$, where

$$|A_1\rangle = \frac{1}{4}(|01111\rangle - |01011\rangle + |10010\rangle + |11001\rangle + |11100\rangle + |11101\rangle - |11000\rangle)$$

$$|A_2\rangle = \frac{1}{4}(|01111\rangle + |01011\rangle - |10010\rangle - |11001\rangle - |11100\rangle + |11101\rangle - |11000\rangle)$$

$$|A_3\rangle = \frac{1}{4}(|01111\rangle + |01011\rangle + |10010\rangle + |11001\rangle + |11100\rangle - |11101\rangle + |11000\rangle)$$

$$|A_4\rangle = \frac{1}{4}(|01111\rangle - |01011\rangle - |10010\rangle - |11001\rangle - |11100\rangle - |11101\rangle + |11000\rangle)$$

$$|A_5\rangle = \frac{1}{4}(|11111\rangle - |11011\rangle + |00010\rangle + |01001\rangle + |01100\rangle + |01101\rangle - |01000\rangle)$$

$$|A_6\rangle = \frac{1}{4}(|11111\rangle + |11011\rangle - |00010\rangle - |01001\rangle - |01100\rangle + |01101\rangle - |01000\rangle)$$

$$|A_7\rangle = \frac{1}{4}(|11111\rangle + |11011\rangle + |00010\rangle + |01001\rangle + |01100\rangle - |01101\rangle + |01000\rangle)$$

$$|A_8\rangle = \frac{1}{4}(|11111\rangle - |11011\rangle - |00010\rangle - |01001\rangle - |01100\rangle - |01101\rangle + |01000\rangle)$$

and

$$\begin{aligned}
 |BC_1\rangle &= \alpha|1\rangle|\Phi_-\rangle + \alpha|0\rangle|\Psi_-\rangle + \beta|0\rangle|\Phi_+\rangle + \beta|1\rangle|\Psi_+\rangle \\
 |BC_2\rangle &= \alpha|1\rangle|\Phi_-\rangle - \alpha|0\rangle|\Psi_-\rangle - \beta|0\rangle|\Phi_+\rangle + \beta|1\rangle|\Psi_+\rangle \\
 |BC_3\rangle &= \alpha|1\rangle|\Phi_-\rangle - \alpha|0\rangle|\Psi_-\rangle + \beta|0\rangle|\Phi_+\rangle - \beta|1\rangle|\Psi_+\rangle \\
 |BC_4\rangle &= \alpha|1\rangle|\Phi_-\rangle + \alpha|0\rangle|\Psi_-\rangle - \beta|0\rangle|\Phi_+\rangle - \beta|1\rangle|\Psi_+\rangle \\
 |BC_5\rangle &= \beta|1\rangle|\Phi_-\rangle + \beta|0\rangle|\Psi_-\rangle + \alpha|0\rangle|\Phi_+\rangle + \alpha|1\rangle|\Psi_+\rangle \\
 |BC_6\rangle &= \beta|1\rangle|\Phi_-\rangle - \beta|0\rangle|\Psi_-\rangle - \alpha|0\rangle|\Phi_+\rangle + \alpha|1\rangle|\Psi_+\rangle \\
 |BC_7\rangle &= \beta|1\rangle|\Phi_-\rangle - \beta|0\rangle|\Psi_-\rangle + \alpha|0\rangle|\Phi_+\rangle - \alpha|1\rangle|\Psi_+\rangle \\
 |BC_8\rangle &= \beta|1\rangle|\Phi_-\rangle + \beta|0\rangle|\Psi_-\rangle - \alpha|0\rangle|\Phi_+\rangle - \alpha|1\rangle|\Psi_+\rangle
 \end{aligned}$$

Bob can now perform a Bell measurement on his particles, and Charlie can obtain a particular resultant state by applying the appropriate unitary operation.

For example, if the joint-state obtained by Bob and Charlie is $\beta|1\rangle|\Phi_-\rangle + \beta|0\rangle|\Psi_-\rangle - \alpha|0\rangle|\Phi_+\rangle - \alpha|1\rangle|\Psi_+\rangle$, one can see that Charlie will obtain the state $|C_i\rangle$, $i = 1, 2, 3, 4$ corresponding to the state measured by Bob $|B_i\rangle$, where $|B_1\rangle = \frac{1}{\sqrt{2}}|01\rangle$, $|B_2\rangle = \frac{1}{\sqrt{2}}|10\rangle$, $|B_3\rangle = \frac{1}{\sqrt{2}}|11\rangle$, $|B_4\rangle = \frac{1}{\sqrt{2}}|00\rangle$ and $|C_1\rangle = \alpha|0\rangle + \beta|1\rangle$, $|C_2\rangle = \alpha|0\rangle - \beta|1\rangle$, $|C_3\rangle = \alpha|1\rangle + \beta|0\rangle$, $|C_4\rangle = \alpha|1\rangle - \beta|0\rangle$

B. Quantum teleportation

B.1 Quantum teleportation of arbitrary one-qubit state

B.1.1 Linear teleportation scheme

To begin with, an arbitrary single qubit state can be teleported using the resource state $|\Gamma_7\rangle$ will be considered. In this case Alice possesses qubits 1, 2, 3, 4, 5, 6 and the 7th particle belongs to Bob. Alice wants to transport an arbitrary state $|\psi^{(1)}\rangle = \alpha|0\rangle + \beta|1\rangle$ to Bob. The combined state of the system is $|\Gamma_7^{(1)}\rangle = |\psi^{(1)}\rangle \otimes |\Gamma_7\rangle$. Alice measures the seven qubits in her possession via the seven qubit orthonormal states:

$$\begin{aligned}
 |\xi^\pm\rangle &= |0000\rangle|\Psi_{GHZ}^0\rangle - |0001\rangle|\Psi_{GHZ}^3\rangle + |0010\rangle|\Psi_{GHZ}^7\rangle \\
 &\quad + |0011\rangle|\Psi_{GHZ}^4\rangle - |0100\rangle|\Psi_{GHZ}^5\rangle - |0101\rangle|\Psi_{GHZ}^6\rangle \\
 &\quad + |0110\rangle|\Psi_{GHZ}^2\rangle + |0111\rangle|\Psi_{GHZ}^1\rangle \pm (|1000\rangle|\Psi_{GHZ}^2\rangle \\
 &\quad - |1001\rangle|\Psi_{GHZ}^1\rangle - |1010\rangle|\Psi_{GHZ}^5\rangle - |1011\rangle|\Psi_{GHZ}^6\rangle \\
 &\quad + |1100\rangle|\Psi_{GHZ}^7\rangle + |1101\rangle|\Psi_{GHZ}^4\rangle + |1110\rangle|\Psi_{GHZ}^0\rangle \\
 &\quad - |1111\rangle|\Psi_{GHZ}^3\rangle)
 \end{aligned} \tag{A4}$$

$$\begin{aligned}
 |\nu^\pm\rangle &= |1000\rangle|\Psi_{GHZ}^0\rangle - |1001\rangle|\Psi_{GHZ}^3\rangle + |1010\rangle|\Psi_{GHZ}^7\rangle \\
 &\quad + |1011\rangle|\Psi_{GHZ}^4\rangle - |1100\rangle|\Psi_{GHZ}^5\rangle - |1101\rangle|\Psi_{GHZ}^6\rangle \\
 &\quad + |1110\rangle|\Psi_{GHZ}^2\rangle + |1111\rangle|\Psi_{GHZ}^1\rangle \pm (|0000\rangle|\Psi_{GHZ}^2\rangle \\
 &\quad - |0001\rangle|\Psi_{GHZ}^1\rangle - |0010\rangle|\Psi_{GHZ}^5\rangle - |0011\rangle|\Psi_{GHZ}^6\rangle \\
 &\quad + |0100\rangle|\Psi_{GHZ}^7\rangle + |0101\rangle|\Psi_{GHZ}^4\rangle + |0110\rangle|\Psi_{GHZ}^0\rangle \\
 &\quad - |0111\rangle|\Psi_{GHZ}^3\rangle)
 \end{aligned} \tag{A5}$$

where $|\Psi_{GHZ}^{0,1}\rangle = \frac{1}{\sqrt{2}}[|000\rangle \pm |111\rangle]$, $|\Psi_{GHZ}^{2,3}\rangle = \frac{1}{\sqrt{2}}[|001\rangle \pm |110\rangle]$, $|\Psi_{GHZ}^{4,5}\rangle = \frac{1}{\sqrt{2}}[|010\rangle \pm |101\rangle]$ and $|\Psi_{GHZ}^{6,7}\rangle = \frac{1}{\sqrt{2}}[|100\rangle \pm |011\rangle]$.

Alice then conveys the outcome of the measurement results to Bob via two classical bits. Bob then applies a suitable unitary operation from the set $I, \sigma_x, i\sigma_y, \sigma_z$ to recover the original state, sent by Alice. In this way, one can teleport an arbitrary single-qubit state using the state $|\Gamma_7\rangle$.

B.1.2 Probabilistic circular teleportation scheme for arbitrary one-qubit states

Not only is the seven-qubit resource state useful for linear and bidirectional teleportation but can also facilitate the probabilistic teleportation of an arbitrary single-qubit states in a circular manner between three network-nodes (users). Let us say we have Alice, Bob and Charlie in the system, with the first qubit used as a control qubit, qubits 1 and 4 given to Alice, qubits 2 and 6 given to Bob and qubits 3 and 7 given to Charlie. Let us say the arbitrary states are $|\psi_A\rangle = \alpha_A|0_A\rangle + \beta_A|1_A\rangle$, $|\psi_B\rangle = \alpha_B|0_B\rangle + \beta_B|1_B\rangle$ and $|\psi_C\rangle = \alpha_C|0_C\rangle + \beta_C|1_C\rangle$. Then, the composite state is given by $|\psi_A\rangle \otimes |\psi_B\rangle \otimes |\psi_C\rangle \otimes |\Gamma_7\rangle_{TA_1B_1C_1A_1B_1C_1}$, where $|\Gamma_7\rangle_T$ is the control qubit. We apply a CNOT gate using the qubits A, B and C of the arbitrary states as the control-qubits and the first qubits of each user as the target-qubit. Let us for simplicity only consider the case where $|\Gamma_7\rangle_T = |0\rangle$.

Let us now measure the first qubits of Alice, Bob and Charlie in the Z-basis. Let us say $|\Gamma_7\rangle_{A_1B_1C_1} = |010\rangle$, then we have the state $|\psi''\rangle = -\frac{1}{4}(|001\rangle |010\rangle)\alpha_A\alpha_B\alpha_C|0_A0_B0_C\rangle + (|100\rangle |111\rangle)\alpha_A\alpha_B\beta_C|0_A0_B1_C\rangle + (|000\rangle + |011\rangle)\alpha_A\beta_B\alpha_C|0_A1_B0_C\rangle + (|101\rangle + |110\rangle)\alpha_A\beta_B\beta_C|0_A1_B1_C\rangle + (|100\rangle |111\rangle)\beta_A\alpha_B\alpha_C|1_A0_B0_C\rangle + (-|001\rangle + |010\rangle)\beta_A\alpha_B\beta_C|1_A0_B1_C\rangle + (-|101\rangle |110\rangle)\beta_A\beta_B\alpha_C|1_A1_B0_C\rangle + (|000\rangle + |011\rangle)\beta_A\beta_B\beta_C|1_A1_B1_C\rangle$. We can now measure the control qubits in the X-basis. So, let us say, we have $|Q_A Q_B Q_C\rangle = |+_A -_B +_C\rangle$, then we obtain the state $|C_1\rangle(|A_1\rangle(-|B_1\rangle + \chi|B_3\rangle - \chi^{-1}|B_4\rangle - |B_2\rangle) + |A_2\rangle(-|B_1\rangle + \chi|B_3\rangle + \chi^{-1}|B_4\rangle + |B_2\rangle)) + |C_2\rangle(|A_1\rangle(-|B_1\rangle - \chi|B_3\rangle - \chi^{-1}|B_4\rangle + |B_2\rangle) + |A_2\rangle(-|B_1\rangle - \chi|B_3\rangle + \chi^{-1}|B_4\rangle - |B_2\rangle)) + |C_3\rangle(|A_1\rangle(|B_4\rangle - \chi|B_2\rangle - \chi^{-1}|B_1\rangle - |B_3\rangle) + |A_2\rangle(|B_4\rangle - \chi|B_2\rangle + \chi^{-1}|B_1\rangle - |B_3\rangle)) + |C_4\rangle(|A_1\rangle(|B_4\rangle + \chi|B_2\rangle - \chi^{-1}|B_1\rangle - |B_3\rangle) + |A_2\rangle(|B_4\rangle + \chi|B_2\rangle + \chi^{-1}|B_1\rangle + |B_3\rangle))$, where $|C_1\rangle = \beta_C|0\rangle + \alpha_C|1\rangle$, $|C_2\rangle = \beta_C|0\rangle - \alpha_C|1\rangle$, $|C_3\rangle = \beta_C|1\rangle + \alpha_C|0\rangle$, $|C_4\rangle = \beta_C|1\rangle - \alpha_C|0\rangle$, $|B_1\rangle = \alpha_B|1\rangle + \beta_B|0\rangle$, $|B_2\rangle = \alpha_B|1\rangle - \beta_B|0\rangle$, $|B_3\rangle = \alpha_B|0\rangle + \beta_B|1\rangle$, $|B_4\rangle = \alpha_B|0\rangle - \beta_B|1\rangle$, $\chi = \frac{a_2}{a_1}$ with $a_1 = \beta_A + \alpha_A$, $a_2 = \alpha_A - \beta_A$, $|A_1\rangle = a_1|0\rangle + a_2|1\rangle$, $|A_2\rangle = a_1|0\rangle - a_2|1\rangle$. Therefore I see that the users can obtain states derived from the original state of the users next to them (Alice \rightarrow Bob \rightarrow Charlie \rightarrow Alice). However, as you can see, this can be done in a probabilistic manner with one of the users not quite obtaining the original state but rather a derivative-state based on the original.

B.2 Quantum teleportation of arbitrary two-qubit state

B.2.1 Linear teleportation scheme

Similarly, an arbitrary two qubit quantum state can be teleported using the resource-state. In this case Alice possesses qubits 1, 2, 3, 4 and 5, and the 6th and 7th particles belong to Bob. Alice wants to transport an arbitrary state $|\psi^{(2)}\rangle = \alpha|00\rangle + \mu|10\rangle + \gamma|01\rangle + \beta|11\rangle$ to Bob. The combined state of the system is $|\Gamma_7^{(2)}\rangle = |\psi^{(2)}\rangle \otimes |\Gamma_7\rangle$,

$$\begin{aligned}
 |\Gamma_7^{(2)}\rangle = & \alpha(A_{00}|00\rangle + A_{01}|01\rangle + A_{10}|10\rangle + A_{11}|11\rangle) \\
 & + \mu(B_{00}|00\rangle + B_{01}|01\rangle + B_{10}|10\rangle + B_{11}|11\rangle) \\
 & + \gamma(C_{00}|00\rangle + C_{01}|01\rangle + C_{10}|10\rangle + C_{11}|11\rangle) \\
 & + \beta(D_{00}|00\rangle + D_{01}|01\rangle + D_{10}|10\rangle + D_{11}|11\rangle)
 \end{aligned} \tag{A6}$$

where

$$\begin{aligned}
 A_{00} &= |0000\rangle|\Psi_{GHZ}^0\rangle + |0001\rangle|\Psi_{GHZ}^4\rangle - |0010\rangle|\Psi_{GHZ}^5\rangle - |0011\rangle|\Psi_{GHZ}^7\rangle, \\
 A_{11} &= |0000\rangle|\Psi_{GHZ}^1\rangle + |0001\rangle|\Psi_{GHZ}^5\rangle|0010\rangle|\Psi_{GHZ}^2\rangle|0011\rangle|\Psi_{GHZ}^7\rangle, \\
 A_{01} &= |0000\rangle|\Psi_{GHZ}^6\rangle - |0001\rangle|\Psi_{GHZ}^2\rangle + |0010\rangle|\Psi_{GHZ}^4\rangle + |0011\rangle|\Psi_{GHZ}^0\rangle, \\
 A_{10} &= -|0000\rangle|\Psi_{GHZ}^7\rangle - |0001\rangle|\Psi_{GHZ}^3\rangle + |0010\rangle|\Psi_{GHZ}^5\rangle + |0011\rangle|\Psi_{GHZ}^1\rangle, \\
 B_{00} &= |1000\rangle|\Psi_{GHZ}^0\rangle + |1001\rangle|\Psi_{GHZ}^4\rangle|1010\rangle|\Psi_{GHZ}^2\rangle + |1011\rangle|\Psi_{GHZ}^6\rangle, \\
 B_{11} &= |1000\rangle|\Psi_{GHZ}^0\rangle + |1001\rangle|\Psi_{GHZ}^5\rangle - |1010\rangle|\Psi_{GHZ}^3\rangle - |1011\rangle|\Psi_{GHZ}^7\rangle, \\
 B_{01} &= |1000\rangle|\Psi_{GHZ}^6\rangle - |1001\rangle|\Psi_{GHZ}^2\rangle + |1010\rangle|\Psi_{GHZ}^4\rangle + |1011\rangle|\Psi_{GHZ}^0\rangle, \\
 B_{10} &= -|1000\rangle|\Psi_{GHZ}^7\rangle - |1001\rangle|\Psi_{GHZ}^3\rangle + |1010\rangle|\Psi_{GHZ}^5\rangle + |1011\rangle|\Psi_{GHZ}^1\rangle, \\
 C_{00} &= |0100\rangle|\Psi_{GHZ}^0\rangle + |0101\rangle|\Psi_{GHZ}^4\rangle - |0110\rangle|\Psi_{GHZ}^3\rangle + |0111\rangle|\Psi_{GHZ}^6\rangle, \\
 C_{11} &= |0100\rangle|\Psi_{GHZ}^1\rangle + |0101\rangle|\Psi_{GHZ}^5\rangle - |0110\rangle|\Psi_{GHZ}^3\rangle - |0111\rangle|\Psi_{GHZ}^7\rangle, \\
 C_{01} &= |0100\rangle|\Psi_{GHZ}^6\rangle - |0101\rangle|\Psi_{GHZ}^2\rangle|0110\rangle|\Psi_{GHZ}^4\rangle + |0111\rangle|\Psi_{GHZ}^0\rangle, \\
 C_{10} &= |0100\rangle|\Psi_{GHZ}^7\rangle - |0101\rangle|\Psi_{GHZ}^3\rangle + |0110\rangle|\Psi_{GHZ}^5\rangle + |0111\rangle|\Psi_{GHZ}^1\rangle, \\
 D_{00} &= |1100\rangle|\Psi_{GHZ}^0\rangle + |1101\rangle|\Psi_{GHZ}^4\rangle - |1110\rangle|\Psi_{GHZ}^2\rangle + |1111\rangle|\Psi_{GHZ}^6\rangle, \\
 D_{11} &= |1100\rangle|\Psi_{GHZ}^1\rangle + |1101\rangle|\Psi_{GHZ}^5\rangle|1110\rangle|\Psi_{GHZ}^3\rangle|1111\rangle|\Psi_{GHZ}^7\rangle, \\
 D_{01} &= |1100\rangle|\Psi_{GHZ}^6\rangle - |1101\rangle|\Psi_{GHZ}^2\rangle + |1110\rangle|\Psi_{GHZ}^4\rangle + |1111\rangle|\Psi_{GHZ}^0\rangle, \\
 D_{10} &= |1100\rangle|\Psi_{GHZ}^6\rangle - |1101\rangle|\Psi_{GHZ}^3\rangle + |1110\rangle|\Psi_{GHZ}^5\rangle + |1111\rangle|\Psi_{GHZ}^1\rangle,
 \end{aligned}$$

where $|\Psi_{GHZ}^{0,1}\rangle = \frac{1}{\sqrt{2}}[|000\rangle \pm |111\rangle]$, $|\Psi_{GHZ}^{2,3}\rangle = \frac{1}{\sqrt{2}}[|001\rangle \pm |110\rangle]$, $|\Psi_{GHZ}^{4,5}\rangle = \frac{1}{\sqrt{2}}[|010\rangle \pm |101\rangle]$ and $|\Psi_{GHZ}^{6,7}\rangle = \frac{1}{\sqrt{2}}[|100\rangle \pm |011\rangle]$. Now, Bob can carry out a combination of unitary operations, according to the given table, to obtain the original state teleported by Alice.

State Obtained by Alice	Unitary Operation by Bob
$A_{01} + B_{11} + C_{00} + D_{01}$	$I \otimes \sigma_x$
$A_{01} + B_{11} - C_{00} - D_{01}$	$\sigma_z \otimes \sigma_x$
$A_{01} - B_{11} + C_{00} - D_{01}$	$I \otimes i\sigma_y$
$A_{01} - B_{11} - C_{00} + D_{01}$	$\sigma_z \otimes i\sigma_y$
$A_{11} + B_{01} + C_{10} + D_{00}$	$\sigma_x \otimes \sigma_x$
$A_{11} - B_{01} + C_{10} - D_{00}$	$\sigma_x \otimes i\sigma_y$
$A_{11} + B_{01} - C_{10} - D_{00}$	$i\sigma_y \otimes \sigma_x$

State Obtained by Alice	Unitary Operation by Bob
$A_{11} - B_{01} - C_{10} + D_{00}$	$i\sigma_y \otimes i\sigma_y$
$A_{00} + B_{10} + C_{01} + D_{11}$	$I \otimes I$
$A_{00} - B_{10} + C_{01} - D_{11}$	$I \otimes \sigma_z$
$A_{00} + B_{10} - C_{01} - D_{11}$	$\sigma_z \otimes I$
$A_{00} - B_{10} - C_{01} + D_{11}$	$\sigma_z \otimes \sigma_z$
$A_{10} + B_{11} + C_{00} + D_{01}$	$\sigma_x \otimes I$
$A_{10} - B_{11} + C_{00} - D_{01}$	$\sigma_x \otimes \sigma_z$
$A_{10} + B_{11} - C_{00} - D_{01}$	$i\sigma_y \otimes I$
$A_{10} - B_{11} - C_{00} + D_{01}$	$i\sigma_y \otimes \sigma_z$

B.2.2 Bidirectional teleportation of arbitrary two-qubit states

The resource-state can also be used for bidirectional quantum teleportation. Bidirectional Controlled Quantum Teleportation (BCQT) protocols have been proposed for multi-qubit resource states, such as five-qubit [81], six-qubit [82, 83], seven-qubit [84–86] and eight-qubit states [87]. Bidirectional Controlled Quantum Teleportation can teleport arbitrary states between two users under the supervision of a third party. Zha et al proposed the first scheme for BCQT of single qubit states using a maximally entangled seven-qubit quantum state [85]. There have been schemes proposed for BCQT that utilise states with the same number of qubits as the quantum channel being used, and thereby realise bidirectional teleportation of arbitrary single-and two-qubit states under the controller Charlie [84, 86].

Let us say Alice and Bob would like to teleport two-qubit states to each other by utilizing the seven-qubit genuinely entangled resource state. We assume the form of the two-qubit states to be

$$|\phi\rangle_{A_1A_2} = \alpha_0|00\rangle + \alpha_1|01\rangle + \alpha_2|10\rangle + \alpha_3|11\rangle \quad (A7)$$

$$|\phi\rangle_{B_1B_2} = \beta_0|00\rangle + \beta_1|01\rangle + \beta_2|10\rangle + \beta_3|11\rangle \quad (A8)$$

For the resource-state, let Alice have the qubits 1,4 and 7, while Bob has the qubits 2, 3 and 6 and Charlie has the qubit 5. The steps for the scheme are as follows:

- Alice measures qubit 7 of the resource state and A_1 in the bell basis.
- Bob measures qubit 2 of the resource state and B_1 in the bell basis.
- Charlie, Alice and Bob measure their qubits in the Z basis.
- Alice and Bob measure their qubits A_2 and B_2 in the X-basis.
- We apply unitary transformations to the composite state to now get Alice's initial arbitrary state in Bob's terminal and Bob's initial arbitrary state in Alice's terminal.

We will now be looking more closely at these steps with a specific one instance to illustrate each step.

Step 1: Alice measures qubit 7 of the resource state and A_1 in the bell basis. If Alice measures $|\psi_+\rangle$, the remainder state is

$$\begin{aligned}
 & \frac{1}{4\sqrt{2}} (|000\rangle|\psi_+\rangle \frac{(\alpha_0|0\rangle_6|0\rangle_{A_2} + \alpha_1|0\rangle_6|1\rangle_{A_2} + \alpha_2|1\rangle_6|0\rangle_{A_2} + \alpha_3|1\rangle_6|1\rangle_{A_2})}{\sqrt{2}} + \\
 & |001\rangle|\phi_-\rangle \frac{(\alpha_0|1\rangle_6|0\rangle_{A_2} + \alpha_1|1\rangle_6|1\rangle_{A_2} + \alpha_2|0\rangle_6|0\rangle_{A_2} + \alpha_3|0\rangle_6|1\rangle_{A_2})}{\sqrt{2}} + \\
 & |010\rangle|\psi_-\rangle \frac{(-\alpha_0|1\rangle_6|0\rangle_{A_2} - \alpha_1|1\rangle_6|1\rangle_{A_2} - \alpha_2|0\rangle_6|0\rangle_{A_2} - \alpha_3|0\rangle_6|1\rangle_{A_2})}{\sqrt{2}} + \\
 & |011\rangle|\phi_+\rangle \frac{(\alpha_0|0\rangle_6|0\rangle_{A_2} + \alpha_1|0\rangle_6|1\rangle_{A_2} - \alpha_2|1\rangle_6|0\rangle_{A_2} - \alpha_3|1\rangle_6|1\rangle_{A_2})}{\sqrt{2}} + \\
 & |100\rangle|\phi_+\rangle \frac{(\alpha_0|1\rangle_6|0\rangle_{A_2} + \alpha_1|1\rangle_6|1\rangle_{A_2} + \alpha_2|0\rangle_6|0\rangle_{A_2} + \alpha_3|0\rangle_6|1\rangle_{A_2})}{\sqrt{2}} + \\
 & |101\rangle|\psi_-\rangle \frac{(-\alpha_0|0\rangle_6|0\rangle_{A_2} - \alpha_1|0\rangle_6|1\rangle_{A_2} - \alpha_2|1\rangle_6|0\rangle_{A_2} - \alpha_3|1\rangle_6|1\rangle_{A_2})}{\sqrt{2}} + \\
 & |110\rangle|\phi_-\rangle \frac{(-\alpha_0|0\rangle_6|0\rangle_{A_2} - \alpha_1|0\rangle_6|1\rangle_{A_2} + \alpha_2|1\rangle_6|0\rangle_{A_2} + \alpha_3|1\rangle_6|1\rangle_{A_2})}{\sqrt{2}} + \\
 & |111\rangle|\psi_+\rangle \frac{(-\alpha_0|1\rangle_6|0\rangle_{A_2} - \alpha_1|1\rangle_6|1\rangle_{A_2} + \alpha_2|0\rangle_6|0\rangle_{A_2} + \alpha_3|0\rangle_6|1\rangle_{A_2})}{\sqrt{2}}) |\phi\rangle_B
 \end{aligned}$$

Alice communicates her result to Bob using a classical channel.

Step 2: Bob measures qubit 2 of the resource state and B_1 in the bell basis. If Bob Measures $|\psi_+\rangle$, the remainder state is

$$\begin{aligned}
 & \frac{1}{2\sqrt{2}} (|000\rangle \frac{(\alpha_0|0\rangle_6|0\rangle_{A_2} + \alpha_1|0\rangle_6|1\rangle_{A_2} + \alpha_2|1\rangle_6|0\rangle_{A_2} + \alpha_3|1\rangle_6|1\rangle_{A_2})}{\sqrt{2}} \\
 & \quad \times \frac{1}{\sqrt{2}} (\beta_0|00\rangle + \beta_1|01\rangle + \beta_2|10\rangle + \beta_3|11\rangle)_{4,B_2} + |001\rangle \\
 & \quad \times \frac{(\alpha_0|1\rangle_6|0\rangle_{A_2} + \alpha_1|1\rangle_6|1\rangle_{A_2} + \alpha_2|0\rangle_6|0\rangle_{A_2} + \alpha_3|0\rangle_6|1\rangle_{A_2})}{\sqrt{2}} \\
 & \quad \times \frac{1}{\sqrt{2}} (\beta_0|00\rangle + \beta_1|01\rangle + \beta_2|10\rangle + \beta_3|11\rangle)_{4,B_2} + |010\rangle \\
 & \quad \times \frac{(\alpha_0|0\rangle_6|0\rangle_{A_2} + \alpha_1|0\rangle_6|1\rangle_{A_2} - \alpha_2|1\rangle_6|0\rangle_{A_2} - \alpha_3|1\rangle_6|1\rangle_{A_2})}{\sqrt{2}} \\
 & \quad \times \frac{1}{\sqrt{2}} (\beta_0|00\rangle + \beta_1|01\rangle + \beta_2|10\rangle + \beta_3|11\rangle)_{4,B_2} + |011\rangle \\
 & \quad \times \frac{(\alpha_0|0\rangle_6|0\rangle_{A_2} + \alpha_1|0\rangle_6|1\rangle_{A_2} - \alpha_2|1\rangle_6|0\rangle_{A_2} - \alpha_3|1\rangle_6|1\rangle_{A_2})}{\sqrt{2}} \\
 & \quad + \frac{1}{\sqrt{2}} (\beta_0|10\rangle + \beta_1|11\rangle + \beta_2|00\rangle + \beta_3|01\rangle)_{4,B_2} + |100\rangle \\
 & \quad \times \frac{(\alpha_0|1\rangle_6|0\rangle_{A_2} + \alpha_1|1\rangle_6|1\rangle_{A_2} + \alpha_2|0\rangle_6|0\rangle_{A_2} + \alpha_3|0\rangle_6|1\rangle_{A_2})}{\sqrt{2}} \\
 & \quad \times \frac{1}{\sqrt{2}} (\beta_0|10\rangle + \beta_1|11\rangle + \beta_2|00\rangle + \beta_3|01\rangle)_{4,B_2} + |101\rangle \\
 & \quad \times \frac{(-\alpha_0|0\rangle_6|0\rangle_{A_2} - \alpha_1|0\rangle_6|1\rangle_{A_2} - \alpha_2|1\rangle_6|0\rangle_{A_2} - \alpha_3|1\rangle_6|1\rangle_{A_2})}{\sqrt{2}}
 \end{aligned}$$

$$\begin{aligned} & \times \frac{1}{\sqrt{2}} (\beta_0|00\rangle + \beta_1|01\rangle - \beta_2|10\rangle - \beta_3|11\rangle)_{4,B_2} + |110\rangle \\ & \times \frac{(-\alpha_0|0\rangle_6|0\rangle_{A_2} - \alpha_1|0\rangle_6|1\rangle_{A_2} + \alpha_2|1\rangle_6|0\rangle_{A_2} + \alpha_3|1\rangle_6|1\rangle_{A_2})}{\sqrt{2}} \\ & \times \frac{1}{\sqrt{2}} (\beta_0|10\rangle + \beta_1|11\rangle - \beta_2|10\rangle - \beta_3|01\rangle)_{4,B_2} + |111\rangle \\ & \times \frac{(-\alpha_0|1\rangle_6|0\rangle_{A_2} - \alpha_1|1\rangle_6|1\rangle_{A_2} + \alpha_2|0\rangle_6|0\rangle_{A_2} + \alpha_3|0\rangle_6|1\rangle_{A_2})}{\sqrt{2}} \\ & \times \frac{1}{\sqrt{2}} (\beta_0|00\rangle + \beta_1|01\rangle + \beta_2|10\rangle + \beta_3|11\rangle)_{4,B_2} \end{aligned}$$

Bob communicates his result via a classical channel to Alice.

Step 3: Charlie, Alice and Bob measure their qubits in the Z-basis. Let us say they all measure 0, we have the

$$\begin{aligned} & \frac{1}{2} (|000\rangle) \frac{(\alpha_0|0\rangle_6|0\rangle_{A_2} + \alpha_1|0\rangle_6|1\rangle_{A_2} + \alpha_2|1\rangle_6|0\rangle_{A_2} + \alpha_3|1\rangle_6|1\rangle_{A_2})}{\sqrt{2}} \\ & \times \frac{1}{\sqrt{2}} (\beta_0|00\rangle + \beta_1|01\rangle + \beta_2|10\rangle + \beta_3|11\rangle)_{4,B_2} \end{aligned} \quad (A9)$$

Step 4: Let Alice apply a CNOT with A_2 as control and qubit 1 as target, and let Bob apply a CNOT with B_2 as control and qubit 3 as target, to get

$$\begin{aligned} & \frac{1}{2\sqrt{2}} (|0\rangle) \frac{(\alpha_0|000\rangle + \alpha_1|101\rangle_{A_2} + \alpha_2|010\rangle + \alpha_3|111\rangle)_{1,6,A_2}}{\sqrt{2}} \\ & \times \frac{1}{\sqrt{2}} (\beta_0|000\rangle + \beta_1|101\rangle + \beta_2|010\rangle + \beta_3|111\rangle)_{3,4,B_2} \end{aligned} \quad (A10)$$

Step 4: Alice and Bob measure their qubits A_2 and B_2 in the X-basis. Let us say they obtain the state $|+\rangle = \frac{1}{\sqrt{2}} (|0\rangle + |1\rangle)$, then the composite state is given by

$$\begin{aligned} & \frac{1}{2} (|0\rangle) \frac{(\alpha_0|00\rangle + \alpha_1|10\rangle_{A_2} + \alpha_2|01\rangle + \alpha_3|11\rangle)_{1,6}}{\sqrt{2}} \\ & \times \frac{1}{\sqrt{2}} (\beta_0|00\rangle + \beta_1|10\rangle + \beta_2|01\rangle + \beta_3|11\rangle)_{3,4} \end{aligned} \quad (A11)$$

Step 5: We apply unitary transformations to the composite state to now get Alice's initial arbitrary state in Bob's terminal and Bob's initial arbitrary state in Alice's terminal. In this instance, the unitary transformation is simply $I \otimes I \otimes I \otimes I$ with I being the identity matrix.

B.3 Quantum teleportation of arbitrary three-qubit state

The seven-qubit resource state can be used for the perfect linear teleportation of an arbitrary three qubit state. In this case, Alice possesses qubits 1, 2, 3, 4 and 5, and the 6th and 7th particles belong to Bob. Alice wants to transport an arbitrary state $|\psi^{(3)}\rangle = a|000\rangle + b|001\rangle + c|010\rangle + d|011\rangle + e|100\rangle + f|101\rangle + g|110\rangle + h|111\rangle$ to Bob. Using the decomposition given in *Supplementary Material*, the states possessed by, and the unitary transforms to be performed by, Bob have been recorded, to

accomplish the teleportation of an arbitrary three-qubit state. A point to note here is that we get the GHZ state for $a = h = \frac{1}{\sqrt{2}}$, $b = c = d = e = f = g = 0$ and the W state for $b = c = e = \frac{1}{\sqrt{3}}$, $a = d = f = g = h = 0$.

The teleportation of an arbitrary three-qubit state using our resource-state has as the initial composite state,

$$\begin{aligned}
 |\Gamma_7^{(3)}\rangle &= |\psi^{(3)}\rangle \otimes |\Gamma_7\rangle \\
 &= aA_{000}|000\rangle + aA_{001}|001\rangle + aA_{010}|010\rangle + aA_{011}|011\rangle \\
 &\quad + aA_{100}|100\rangle + aA_{101}|101\rangle + aA_{110}|110\rangle + aA_{111}|111\rangle \\
 &\quad + bB_{000}|000\rangle + bB_{001}|001\rangle + bB_{010}|010\rangle + bB_{011}|011\rangle \\
 &\quad + bB_{100}|100\rangle + bB_{101}|101\rangle + bB_{110}|110\rangle + bB_{111}|111\rangle \\
 &\quad + cC_{000}|000\rangle + cC_{001}|001\rangle + cC_{010}|010\rangle + cC_{011}|011\rangle \\
 &\quad + cC_{100}|100\rangle + cC_{101}|101\rangle + cC_{110}|110\rangle + cC_{111}|111\rangle \\
 &\quad + dD_{000}|000\rangle + dD_{001}|001\rangle + dD_{010}|010\rangle + dD_{011}|011\rangle \\
 &\quad + dD_{100}|100\rangle + dD_{101}|101\rangle + dD_{110}|110\rangle + dD_{111}|111\rangle \\
 &\quad + eE_{000}|000\rangle + eE_{001}|001\rangle + eE_{010}|010\rangle + eE_{011}|011\rangle \\
 &\quad + eE_{100}|100\rangle + eE_{101}|101\rangle + eE_{110}|110\rangle + eE_{111}|111\rangle \\
 &\quad + fF_{000}|000\rangle + fF_{001}|001\rangle + fF_{010}|010\rangle + fF_{011}|011\rangle \\
 &\quad + fF_{100}|100\rangle + fF_{101}|101\rangle + fF_{110}|110\rangle + fF_{111}|111\rangle \\
 &\quad + gG_{000}|000\rangle + gG_{001}|001\rangle + gG_{010}|010\rangle + gG_{011}|011\rangle \\
 &\quad + gG_{100}|100\rangle + gG_{101}|101\rangle + gG_{110}|110\rangle + gG_{111}|111\rangle \\
 &\quad + hH_{000}|000\rangle + hH_{001}|001\rangle + hH_{010}|010\rangle + hH_{011}|011\rangle \\
 &\quad + hH_{100}|100\rangle + hH_{101}|101\rangle + hH_{110}|110\rangle + hH_{111}|111\rangle
 \end{aligned} \tag{A12}$$

with

$$\begin{aligned}
 |A_{000}\rangle &= |0000000\rangle + |0000101\rangle - |0001011\rangle + |0001110\rangle \\
 |A_{001}\rangle &= |0000010\rangle + |0001001\rangle + |0001100\rangle - |0000111\rangle \\
 |A_{010}\rangle &= |0000111\rangle - |0000010\rangle + |0001001\rangle + |0001100\rangle \\
 |A_{011}\rangle &= |0000000\rangle + |0000101\rangle + |0001011\rangle - |0001110\rangle \\
 |A_{100}\rangle &= |0000011\rangle + |0000110\rangle - |0001000\rangle + |0001101\rangle \\
 |A_{101}\rangle &= |0000001\rangle - |0000100\rangle + |0001010\rangle + |0001111\rangle \\
 |A_{110}\rangle &= |0000001\rangle - |0000100\rangle - |0001010\rangle - |0001111\rangle \\
 |A_{111}\rangle &= |0001101\rangle - |0000011\rangle - |0000110\rangle - |0001000\rangle
 \end{aligned}$$

$$\begin{aligned}
 |B_{000}\rangle &= |0010000\rangle + |0010101\rangle - |0011011\rangle + |0011110\rangle \\
 |B_{001}\rangle &= |0010010\rangle + |0011001\rangle + |0011100\rangle - |0010111\rangle \\
 |B_{010}\rangle &= |0010111\rangle - |0010010\rangle + |0011001\rangle + |0011100\rangle \\
 |B_{011}\rangle &= |0010000\rangle + |0010101\rangle + |0011011\rangle - |0011110\rangle \\
 |B_{100}\rangle &= |0010011\rangle + |0010110\rangle - |0011000\rangle + |0011101\rangle \\
 |B_{101}\rangle &= |0010001\rangle - |0010100\rangle + |0011010\rangle + |0011111\rangle \\
 |B_{110}\rangle &= |0010001\rangle - |0010100\rangle - |0011010\rangle - |0011111\rangle \\
 |B_{111}\rangle &= |0011101\rangle - |0010011\rangle - |0010110\rangle - |0011000\rangle \\
 |C_{000}\rangle &= |0100000\rangle + |0100101\rangle - |0101011\rangle + |0101110\rangle \\
 |C_{001}\rangle &= |0100010\rangle + |0101001\rangle + |0101100\rangle - |0100111\rangle \\
 |C_{010}\rangle &= |0100111\rangle - |0100010\rangle + |0101001\rangle + |0101100\rangle \\
 |C_{011}\rangle &= |0100000\rangle + |0100101\rangle + |0101011\rangle - |0101110\rangle \\
 |C_{100}\rangle &= |0100011\rangle + |0100110\rangle - |0101000\rangle + |0101101\rangle \\
 |C_{101}\rangle &= |0100001\rangle - |0100100\rangle + |0101010\rangle + |0101111\rangle \\
 |C_{110}\rangle &= |0100001\rangle - |0100100\rangle - |0101010\rangle - |0101111\rangle \\
 |C_{111}\rangle &= |0101101\rangle - |0100011\rangle - |0100110\rangle - |0101000\rangle \\
 |D_{000}\rangle &= |0110000\rangle + |0110101\rangle - |0111011\rangle + |0111110\rangle \\
 |D_{001}\rangle &= |0110010\rangle + |0111001\rangle + |0111100\rangle - |0110111\rangle \\
 |D_{010}\rangle &= |0110111\rangle - |0110010\rangle + |0111001\rangle + |0111100\rangle \\
 |D_{011}\rangle &= |0110000\rangle + |0110101\rangle + |0111011\rangle - |0111110\rangle \\
 |D_{100}\rangle &= |0110011\rangle + |0110110\rangle - |0111000\rangle + |0111101\rangle \\
 |D_{101}\rangle &= |0110001\rangle - |0110100\rangle + |0111010\rangle + |0111111\rangle \\
 |D_{110}\rangle &= |0110001\rangle - |0110100\rangle - |0111010\rangle - |0111111\rangle \\
 |D_{111}\rangle &= |0111101\rangle - |0110011\rangle - |0110110\rangle - |0111000\rangle \\
 |E_{000}\rangle &= |1000000\rangle + |1000101\rangle - |1001011\rangle + |1001110\rangle \\
 |E_{001}\rangle &= |1000010\rangle + |1001001\rangle + |1001100\rangle - |1000111\rangle \\
 |E_{010}\rangle &= |1000111\rangle - |1000010\rangle + |10001001\rangle + |10001100\rangle \\
 |E_{011}\rangle &= |1000000\rangle + |1000101\rangle + |1001011\rangle - |1001110\rangle \\
 |E_{100}\rangle &= |1000011\rangle + |1000110\rangle - |1001000\rangle + |1001101\rangle \\
 |E_{101}\rangle &= |1000001\rangle - |1000100\rangle + |1001010\rangle + |1001111\rangle \\
 |E_{110}\rangle &= |1000001\rangle - |1000100\rangle - |1001010\rangle - |1001111\rangle \\
 |E_{111}\rangle &= |1001101\rangle - |1000011\rangle - |1000110\rangle - |1001000\rangle \\
 |F_{000}\rangle &= |1010000\rangle + |1010101\rangle - |1011011\rangle + |1011110\rangle \\
 |F_{001}\rangle &= |1010010\rangle + |1011001\rangle + |1011100\rangle - |1010111\rangle \\
 |F_{010}\rangle &= |1010111\rangle - |1010010\rangle + |1011001\rangle + |1011100\rangle \\
 |F_{011}\rangle &= |1010000\rangle + |1010101\rangle + |1011011\rangle - |1011110\rangle \\
 |F_{100}\rangle &= |1010011\rangle + |1010110\rangle - |1011000\rangle + |1011101\rangle \\
 |F_{101}\rangle &= |1010001\rangle - |1010100\rangle + |1011010\rangle + |1011111\rangle \\
 |F_{110}\rangle &= |1010001\rangle - |1010100\rangle - |1011010\rangle - |1011111\rangle \\
 |F_{111}\rangle &= |1011101\rangle - |1010011\rangle - |1010110\rangle - |1011000\rangle
 \end{aligned}$$

$$\begin{aligned}
 |G_{000}\rangle &= |1100000\rangle + |1100101\rangle - |1101011\rangle + |1101110\rangle \\
 |G_{001}\rangle &= |1100010\rangle + |1101001\rangle + |1101100\rangle - |1100111\rangle \\
 |G_{010}\rangle &= |1100111\rangle - |1100010\rangle + |1101001\rangle + |1101100\rangle \\
 |G_{011}\rangle &= |1100000\rangle + |1100101\rangle + |1101011\rangle - |1101110\rangle \\
 |G_{100}\rangle &= |1100011\rangle + |1100110\rangle - |1101000\rangle + |1101101\rangle \\
 |G_{101}\rangle &= |1100001\rangle - |1100100\rangle + |1101010\rangle + |1101111\rangle \\
 |G_{110}\rangle &= |1100001\rangle - |1100100\rangle - |1101010\rangle - |1101111\rangle \\
 |G_{111}\rangle &= |1101101\rangle - |1100011\rangle - |0000110\rangle - |0001000\rangle \\
 |H_{000}\rangle &= |11110000\rangle + |11110101\rangle - |11111011\rangle + |11111110\rangle \\
 |H_{001}\rangle &= |11110010\rangle + |11111001\rangle + |11111100\rangle - |11110111\rangle \\
 |H_{010}\rangle &= |11110111\rangle - |11110010\rangle + |11111001\rangle + |11111100\rangle \\
 |H_{011}\rangle &= |11110000\rangle + |11110101\rangle + |11111011\rangle - |11111110\rangle \\
 |H_{100}\rangle &= |11110011\rangle + |11110110\rangle - |11111000\rangle + |11111101\rangle \\
 |H_{101}\rangle &= |11110001\rangle - |11110100\rangle + |11111010\rangle + |11111111\rangle \\
 |H_{110}\rangle &= |11110001\rangle - |11110100\rangle - |11111010\rangle - |11111111\rangle \\
 |H_{111}\rangle &= |11111101\rangle - |11110011\rangle - |11110110\rangle - |11111000\rangle
 \end{aligned}$$

An arbitrary three qubit state can be decomposed in terms of these basis-vectors,

$$\begin{aligned}
 &(a|000\rangle + b|001\rangle + c|010\rangle + d|011\rangle + e|100\rangle \\
 &+ f|101\rangle + g|110\rangle + h|111\rangle)|\Psi_7\rangle \\
 &= \sum_{\text{permutations}} ((-1)^{I_1} A_{a_1 a_2 a_3} + (-1)^{I_2} B_{b_1 b_2 b_3} \\
 &+ (-1)^{I_3} C_{c_1 c_2 c_3} + (-1)^{I_4} D_{d_1 d_2 d_3} \\
 &+ (-1)^{I_5} E_{e_1 e_2 e_3} + (-1)^{I_6} F_{f_1 f_2 f_3} \\
 &+ (-1)^{I_7} G_{g_1 g_2 g_3} + (-1)^{I_8} H_{h_1 h_2 h_3}) \\
 &((-1)^{I_1} a|a_1 a_2 a_3\rangle + (-1)^{I_2} b|b_1 b_2 b_3\rangle \\
 &+ (-1)^{I_3} c|c_1 c_2 c_3\rangle + (-1)^{I_4} d|d_1 d_2 d_3\rangle \\
 &+ (-1)^{I_5} e|e_1 e_2 e_3\rangle + (-1)^{I_6} f|f_1 f_2 f_3\rangle \\
 &+ (-1)^{I_7} g|g_1 g_2 g_3\rangle + (-1)^{I_8} h|h_1 h_2 h_3\rangle)
 \end{aligned} \tag{A13}$$

where I_i ($i = 1, 2, 3, 4, 5, 6, 7, 8$) can take values 0 or 1 independently, and L_j ($L = a, b, c, d, e, f, g, h; j = 1, 2, 3$) can take values 0 or 1 independently. The summation is over all possible permutation states obtained.

The relevant transformations for the three-qubit teleportation are given in terms of the following basic operations:

Projection of i^{th} component P_i :

$$P_1 = \begin{pmatrix} 10 \\ 00 \end{pmatrix} \quad P_2 = \begin{pmatrix} 00 \\ 01 \end{pmatrix} \tag{A14}$$

Flip and Projection of i^{th} component F_i :

$$F_1 = \begin{pmatrix} 01 \\ 00 \end{pmatrix} \quad F_2 = \begin{pmatrix} 00 \\ 10 \end{pmatrix} \tag{A15}$$

State Obtained by Alice	Short-Hand Form of Transformation
$-A_{111} + B_{110} - C_{101} - D_{100} + E_{011} + F_{010} + G_{001} + H_{000}$	$I\sigma_y \otimes F_1 \otimes F_1 - \sigma_x \otimes F_2 \otimes F_1 + \sigma_x \otimes \sigma_x \otimes F_2$
$A_{111} - B_{110} - C_{101} - D_{100} + E_{011} + F_{010} + G_{001} + H_{000}$	$-I\sigma_y \otimes F_1 \otimes F_1 - \sigma_x \otimes F_2 \otimes F_1 + \sigma_x \otimes \sigma_x \otimes F_2$
$-A_{111} - B_{110} - C_{101} - D_{100} + E_{011} + F_{010} + G_{001} + H_{000}$	$-\sigma_x \otimes \sigma_x \otimes F_1 + \sigma_x \otimes \sigma_x \otimes F_2$

IntechOpen

IntechOpen

Author details

Mrittunjoy Guha Majumdar
 Indian Institute of Science, Bangalore, India

*Address all correspondence to: mrittunjoyguhamajumdar@hotmail.com

IntechOpen

© 2021 The Author(s). Licensee IntechOpen. This chapter is distributed under the terms of the Creative Commons Attribution License (<http://creativecommons.org/licenses/by/3.0>), which permits unrestricted use, distribution, and reproduction in any medium, provided the original work is properly cited. 

References

- [1] C. H. Bennett, G. Brassard, C. Crépeau, R. Jozsa, A. Peres, and W. K. Wootters, Teleporting an unknown quantum state via dual classical and einstein-podolskyrosen channels, *Physical review letters* **70**, 1895 (1993).
- [2] W. Tian-Yin and W. Qiao-Yan, Controlled quantum teleportation with bell states, *Chinese Physics B* **20**, 040307 (2011).
- [3] X. Tan, X. Li, and P. Yang, Perfect quantum teleportation via bell states, *Computers, Materials & Continua* **57**, 495 (2018).
- [4] J. Dong and J. Teng, Controlled teleportation of an arbitrary n-qudit state using nonmaximally entangled ghz states, *The European Physical Journal D* **49**, 129 (2008).
- [5] S. Hassanpour and M. Houshmand, Bidirectional teleportation of a pure epr state by using ghz states, *Quantum Information Processing* **15**, 905 (2016).
- [6] X. Gao, Z. Zhang, Y. Gong, B. Sheng, and X. Yu, Teleportation of entanglement using a three-particle entangled w state, *JOSA B* **34**, 142 (2017).
- [7] B.-S. Shi and A. Tomita, Teleportation of an unknown state by w state, *Physics Letters A* **296**, 161 (2002).
- [8] P. Espoukeh and P. Pedram, Quantum teleportation through noisy channels with multi-qubit ghz states, *Quantum information processing* **13**, 1789 (2014).
- [9] R.-G. Zhou, C. Qian, and H. Ian, Cyclic and bidirectional quantum teleportation via pseudo multi-qubit states, *IEEE Access* **7**, 42445 (2019).
- [10] A. Kumar, S. Adhikari, S. Banerjee, and S. Roy, Optimal quantum communication using multiparticle partially entangled states, *Physical Review A* **87**, 022307 (2013).
- [11] X.-Z. Zhou, X.-T. Yu, and Z.-C. Zhang, Multi-hop teleportation of an unknown qubit state based on w states, *International Journal of Theoretical Physics* **57**, 981 (2018).
- [12] D. Joy and M. Sabir, Efficient schemes for the quantum teleportation of a sub-class of tripartite entangled states, *Quantum Information Processing* **17**, 170 (2018).
- [13] Q. Quan, M.-J. Zhao, S.-M. Fei, H. Fan, W.-L. Yang, and G.-L. Long, Two-copy quantum teleportation, *Scientific reports* **8**, 1 (2018).
- [14] S. Rajiuddin, A. Baishya, B. K. Behera, and P. K. Panigrahi, Experimental realization of quantum teleportation of an arbitrary two-qubit state using a four-qubit cluster state, *Quantum Information Processing* **19**, 87 (2020).
- [15] Y.-H. Luo, H.-S. Zhong, M. Erhard, X.-L. Wang, L.-C. Peng, M. Krenn, X. Jiang, L. Li, N.-L. Liu, C.-Y. Lu, et al., Quantum teleportation in high dimensions, *Physical review letters* **123**, 070505 (2019).
- [16] K. Hofmann, A. Semenov, W. Vogel, and M. Bohmann, Quantum teleportation through atmospheric channels, *Physica Scripta* **94**, 125104 (2019).
- [17] V. Sharma, C. Shukla, S. Banerjee, and A. Pathak, Controlled bidirectional remote state preparation in noisy environment: a generalized view, *Quantum Information Processing* **14**, 3441 (2015).
- [18] Y.-J. Duan, X.-W. Zha, X.-M. Sun, and J.-F. Xia, Bidirectional quantum controlled teleportation via a maximally

seven-qubit entangled state, *International Journal of Theoretical Physics* **53**, 2697 (2014).

[19] F.-G. Deng, C.-Y. Li, Y.-S. Li, H.-Y. Zhou, and Y. Wang, Symmetric multiparty-controlled teleportation of an arbitrary two-particle entanglement, *Physical Review A* **72**, 022338 (2005).

[20] F. Yan and D. Wang, Probabilistic and controlled teleportation of unknown quantum states, *Physics Letters A* **316**, 297 (2003).

[21] Z.-j. Zhang and C.-Y. Cheung, Shared quantum remote control: quantum operation sharing, *Journal of Physics B: Atomic, Molecular and Optical Physics* **44**, 165508 (2011).

[22] Q. Ji, Y. Liu, X. Yin, X. Liu, and Z. Zhang, Quantum operation sharing with symmetric and asymmetric w states, *Quantum information processing* **12**, 2453 (2013).

[23] M. Hillery, V. Bužek, and A. Berthiaume, Quantum secret sharing, *Physical Review A* **59**, 1829 (1999).

[24] L. Xiao, G. L. Long, F.-G. Deng, and J.-W. Pan, Efficient multiparty quantum-secret-sharing schemes, *Physical Review A* **69**, 052307 (2004).

[25] D. Gottesman, Theory of quantum secret sharing, *Physical Review A* **61**, 042311 (2000).

[26] J. Heo, C.-H. Hong, M.-S. Kang, H. Yang, H.-J. Yang, J.-P. Hong, and S.-G. Choi, Implementation of controlled quantum teleportation with an arbitrator for secure quantum channels via quantum dots inside optical cavities, *Scientific reports* **7**, 1 (2017).

[27] T. Zheng, Y. Chang, and S.-B. Zhang, Arbitrated quantum signature scheme with quantum teleportation by using two three-qubit ghz states,

Quantum Information Processing **19**, 1 (2020).

[28] M. Walter, D. Gross, and J. Eisert, Multipartite entanglement, *Quantum Information: From Foundations to Quantum Technology Applications*, **293** (2016).

[29] T. Dash, R. Sk, and P. K. Panigrahi, Deterministic joint remote state preparation of arbitrary two-qubit state through noisy cluster-ghz channel, *Optics Communications* **464**, 125518 (2020).

[30] Z.-Z. Zou, X.-T. Yu, Y.-X. Gong, and Z.-C. Zhang, Multihop teleportation of two-qubit state via the composite ghz–bell channel, *Physics Letters A* **381**, 76 (2017).

[31] S. Shuai, N. Chen, and B. Yan, Bidirectional quantum communication through the composite ghz-ghz channel, *Applied Sciences* **10**, 5500 (2020).

[32] Y.-y. Nie, Y.-h. Li, X.-p. Wang, and M.-h. Sang, Controlled dense coding using a five-atom cluster state in cavity qed, *Quantum information processing* **12**, 1851 (2013).

[33] X.-J. Yi and J.-M. Wang, Spin squeezing of superposition of multi-qubit ghz state and w state, *International Journal of Theoretical Physics* **50**, 2520 (2011).

[34] L. Chen and Y.-X. Chen, Classification of ghz-type, w-type, and ghz-w-type multiqubit entanglement, *Physical Review A* **74**, 062310 (2006).

[35] Z.-X. Man, Y.-J. Xia, and N. B. An, Genuine multiqubit entanglement and controlled teleportation, *Physical Review A* **75**, 052306 (2007).

[36] C.-P. Yang, Q.-P. Su, Y. Zhang, and F. Nori, Implementing a multi-target-qubit controlled-not gate with logical qubits outside a decoherence-free

subspace and its application in creating quantum entangled states, *Physical Review A* **101**, 032329 (2020).

[37] P. Contreras-Tejada, C. Palazuelos, and J. I. De Vicente, Resource theory of entanglement with a unique multipartite maximally entangled state, *Physical Review Letters* **122**, 120503 (2019).

[38] T. Theurer, N. Killoran, D. Egloff, and M. B. Plenio, Resource theory of superposition, *Physical review letters* **119**, 230401 (2017).

[39] S. Bäuml, S. Das, X. Wang, and M. M. Wilde, Resource theory of entanglement for bipartite quantum channels, arXiv preprint arXiv: 1907.04181 (2019).

[40] F. Shahandeh, The resource theory of entanglement, in *Quantum Correlations* (Springer, 2019) pp. 61–109.

[41] D. A. Lidar, I. L. Chuang, and K. B. Whaley, Decoherence-free subspaces for quantum computation, *Physical Review Letters* **81**, 2594 (1998).

[42] D. Bacon, J. Kempe, D. A. Lidar, and K. B. Whaley, Universal fault-tolerant quantum computation on decoherence-free subspaces, *Physical Review Letters* **85**, 1758 (2000).

[43] P. G. Kwiat, A. J. Berglund, J. B. Altepeter, and A. G. White, Experimental verification of decoherence-free subspaces, *Science* **290**, 498 (2000).

[44] D. A. Lidar and K. B. Whaley, Decoherence-free subspaces and subsystems, in *Irreversible quantum dynamics* (Springer, 2003) pp. 83–120.

[45] J. Roffe, Quantum error correction: an introductory guide, *Contemporary Physics* **60**, 226 (2019).

[46] R. Raussendorf and J. Harrington, Fault-tolerant quantum computation with high threshold in two dimensions, *Physical review letters* **98**, 190504 (2007).

[47] R. Cleve, Quantum stabilizer codes and classical linear codes, *Physical Review A* **55**, 4054 (1997).

[48] D. Gottesman, Stabilizer codes and quantum error correction, arXiv preprint quant-ph/9705052 (1997).

[49] R. Raussendorf and H. J. Briegel, A one-way quantum computer, *Physical Review Letters* **86**, 5188 (2001).

[50] S. Bravyi and R. Raussendorf, Measurement-based quantum computation with the toric code states, *Physical Review A* **76**, 022304 (2007).

[51] R. Raussendorf, D. E. Browne, and H. J. Briegel, Measurement-based quantum computation on cluster states, *Physical review A* **68**, 022312 (2003).

[52] H. J. Briegel and R. Raussendorf, Persistent entanglement in arrays of interacting particles, *Physical Review Letters* **86**, 910 (2001).

[53] T. J. Osborne and F. Verstraete, General monogamy inequality for bipartite qubit entanglement, *Physical review letters* **96**, 220503 (2006).

[54] X.-N. Zhu and S.-M. Fei, Entanglement monogamy relations of qubit systems, *Physical Review A* **90**, 024304 (2014).

[55] Y.-K. Bai, M.-Y. Ye, and Z. Wang, Entanglement monogamy and entanglement evolution in multipartite systems, *Physical Review A* **80**, 044301 (2009).

[56] M. Koashi and A. Winter, Monogamy of quantum entanglement and other correlations, *Physical Review A* **69**, 022309 (2004).

- [57] Z.-X. Jin and S.-M. Fei, Tighter entanglement monogamy relations of qubit systems, *Quantum Information Processing* **16**, 77 (2017).
- [58] C. Di Franco, M. Paternostro, and M. Kim, Nested entangled states for distributed quantum channels, *Physical Review A* **77**, 020303 (2008).
- [59] F. Fröwis and W. Dür, Stable macroscopic quantum superpositions, *Physical review letters* **106**, 110402 (2011).
- [60] M. Christandl, N. Datta, A. Ekert, and A. J. Landahl, Perfect state transfer in quantum spin networks, *Physical review letters* **92**, 187902 (2004).
- [61] M. Christandl, N. Datta, T. C. Dorlas, A. Ekert, A. Kay, and A. J. Landahl, Perfect transfer of arbitrary states in quantum spin networks, *Physical Review A* **71**, 032312 (2005).
- [62] D. Saha and P. K. Panigrahi, N-qubit quantum teleportation, information splitting and superdense coding through the composite ghz–bell channel, *Quantum Information Processing* **11**, 615 (2012).
- [63] S. Zippilli, J. Li, and D. Vitali, Steady-state nested entanglement structures in harmonic chains with single-site squeezing manipulation, *Physical Review A* **92**, 032319 (2015).
- [64] A. G. Fowler, A. M. Stephens, and P. Groszkowski, Highthreshold universal quantum computation on the surface code, *Physical Review A* **80**, 052312 (2009).
- [65] D. S. Wang, A. G. Fowler, and L. C. Hollenberg, Surface code quantum computing with error rates over 1%, *Physical Review A* **83**, 020302 (2011).
- [66] H. Bombín and M. A. Martin-Delgado, Quantum measurements and gates by code deformation, *Journal of Physics A: Mathematical and Theoretical* **42**, 095302 (2009).
- [67] H. Bombin, Clifford gates by code deformation, *New Journal of Physics* **13**, 043005 (2011).
- [68] E. Dennis, A. Kitaev, A. Landahl, and J. Preskill, Topological quantum memory, *Journal of Mathematical Physics* **43**, 4452 (2002).
- [69] M. Mhalla and S. Perdrix, Graph states, pivot minor, and universality of (x, z) -measurements, arXiv preprint arXiv:1202.6551 (2012).
- [70] R. Beals, S. Brierley, O. Gray, A. W. Harrow, S. Kutin, N. Linden, D. Shepherd, and M. Stather, Efficient distributed quantum computing, *Proceedings of the Royal Society A: Mathematical, Physical and Engineering Sciences* **469**, 20120686 (2013).
- [71] D. Bruß and N. Lütkenhaus, Quantum key distribution: from principles to practicalities, *Applicable Algebra in Engineering, Communication and Computing* **10**, 383 (2000).
- [72] P. Komar, E. M. Kessler, M. Bishof, L. Jiang, A. S. Sørensen, J. Ye, and M. D. Lukin, A quantum network of clocks, *Nature Physics* **10**, 582 (2014).
- [73] Z. Eldredge, M. Foss-Feig, J. A. Gross, S. L. Rolston, and A. V. Gorshkov, Optimal and secure measurement protocols for quantum sensor networks, *Physical Review A* **97**, 042337 (2018).
- [74] T. Proctor, P. Knott, and J. Dunningham, Networked quantum sensing, arXiv preprint arXiv:1702.04271 (2017).
- [75] W. Ge, K. Jacobs, Z. Eldredge, A. V. Gorshkov, and M. Foss-Feig, Distributed quantum metrology with linear networks and separable inputs,

Physical review letters **121**, 043604 (2018).

[76] V. Kuzmin, D. Vasilyev, N. Sangouard, W. Dür, and C. Muschik, Scalable repeater architectures for multipartite states, *npj Quantum Information* **5**, 1 (2019).

[77] M. G. Majumdar and S. S. Garani, Quantum network recovery from multinode failure using network encoding with ghz-states on higher-order butterfly networks, *arXiv preprint arXiv:2101.01541* (2021).

[78] X.-W. Zha, H.-Y. Song, J.-X. Qi, D. Wang, and Q. Lan, A genuine maximally seven-qubit entangled state, *arXiv preprint arXiv:1110.5011* (2011).

[79] I. D. Brown, S. Stepney, A. Sudbery, and S. L. Braunstein, Searching for highly entangled multi-qubit states, *Journal of Physics A: Mathematical and General* **38**, 1119 (2005).

[80] A. Borras, A. Plastino, J. Batle, C. Zander, M. Casas, and A. Plastino, Multiqubit systems: highly entangled states and entanglement distribution, *Journal of Physics A: Mathematical and Theoretical* **40**, 13407 (2007).

[81] Y. Chen, Bidirectional controlled quantum teleportation by using five-qubit entangled state, *International Journal of Theoretical Physics* **53**, 1454 (2014).

[82] X. Tan, X. Zhang, and T. Song, Deterministic quantum teleportation of a particular six-qubit state using six-qubit cluster state, *International Journal of Theoretical Physics* **55**, 155 (2016).

[83] R.-G. Zhou, R. Xu, and H. Lan, Bidirectional quantum teleportation by using six-qubit cluster state, *IEEE Access* **7**, 44269 (2019).

[84] M.-h. Sang, Bidirectional quantum controlled teleportation by using a

seven-qubit entangled state, *International Journal of Theoretical Physics* **55**, 380 (2016).

[85] Y.-J. Duan, X.-W. Zha, X.-M. Sun, and J.-F. Xia, Bidirectional quantum controlled teleportation via a maximally seven-qubit entangled state, *International Journal of Theoretical Physics* **53**, 2697 (2014).

[86] W.-q. Hong, Asymmetric bidirectional controlled teleportation by using a seven-qubit entangled state, *International Journal of Theoretical Physics* **55**, 384 (2016).

[87] M. S. S. Zadeh, M. Houshmand, and H. Aghababa, Bidirectional teleportation of a two-qubit state by using eight-qubit entangled state as a quantum channel, *International Journal of Theoretical Physics* **56**, 2101 (2017).